Bayesian Inference for Localization, Sensing and Mapping with Learned Models: A Graphical-Model Perspective

Erik Leitinger

Institute of Communication Networks and Satellite Communications
TU Graz

Focus Period Linköping University 2026:
Wireless Sensing Technologies for Emerging Applications

April 20, 2026

Outline

- Radio Signal-based Localization
- Multipath-based SLAM
- Graphical Models and Message Passing
- Applications:
  - Adaptive MP-SLAM: D-MIMO
  - Direct MP-SLAM: D-MIMO and coherent XL-MIMO
- Hybrid Bayesian Inference with Learned Models

Radio Signal-based Localization

5G/6G wireless communication networks ⇒ signal parameters for localization and sensing

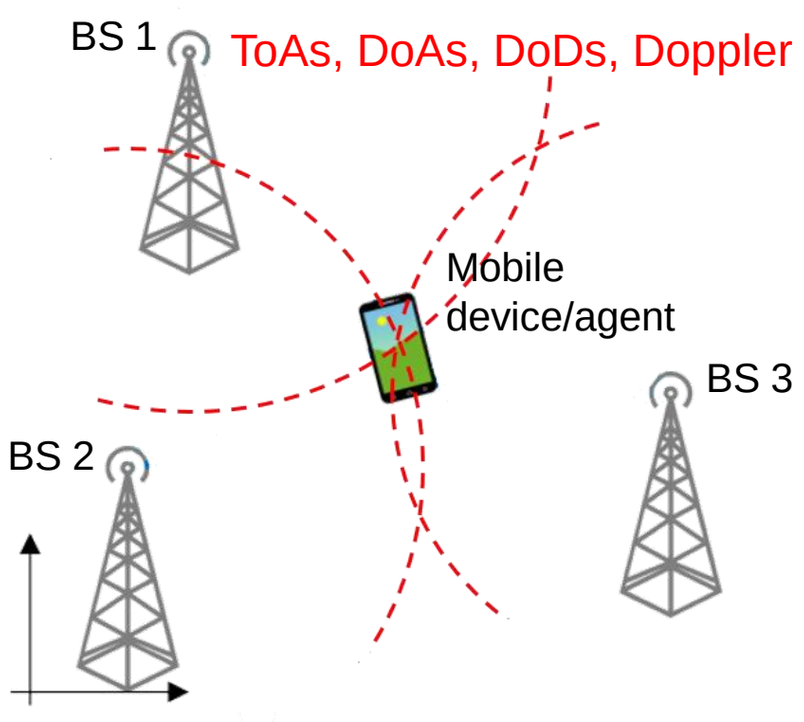

- Uses local infrastructure of **wireless communication networks**
  - Network base stations (BSs) are **physical anchors (PAs)** with known positions
  - ToAs, DoAs, DoDs, Doppler of LOS paths are used for localization
- **Challenges:**
  - Not only LOS ⇒ **multipath propagation**
  - Blocked direct path ⇒ **obstructed LOS (OLOS)**

H. Wymeersch and G. Seco-Granados, "Radio Localization and Sensing—Part I: Fundamentals," in *IEEE Communications Letters*, vol. 26, no. 12, pp. 2816-2820, Dec. 2022, doi: 10.1109/LCOMM.2022.3206821.

What is Multipath-based SLAM?

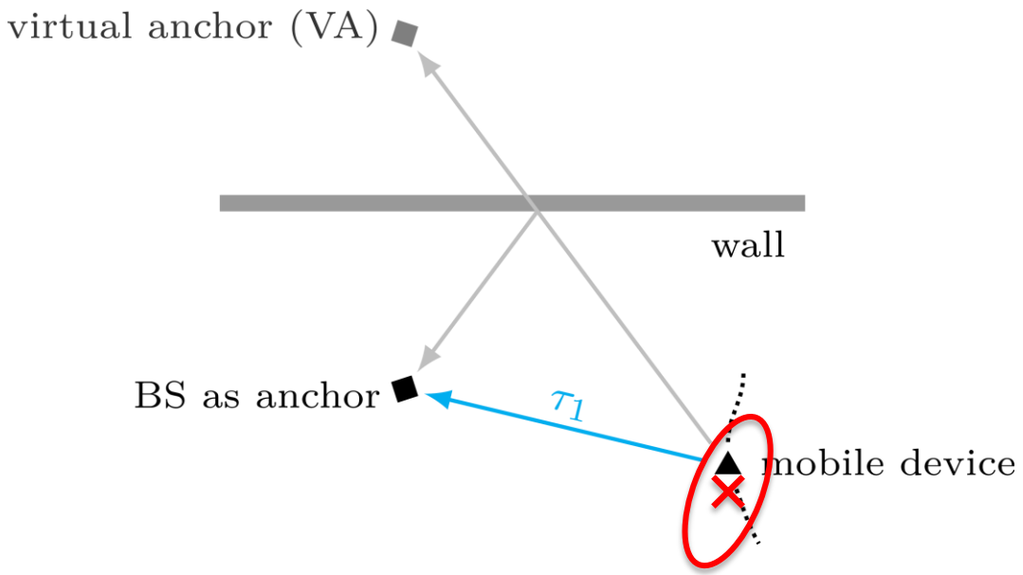

No virtual anchors (VAs) are used

- **MP-SLAM:** Jointly estimates the mobile device position and the propagation environment by exploiting multipath propagation.
- **Virtual anchors (VAs):** Model specular reflections via mirror images of physical anchors (PAs)

What is Multipath-based SLAM?

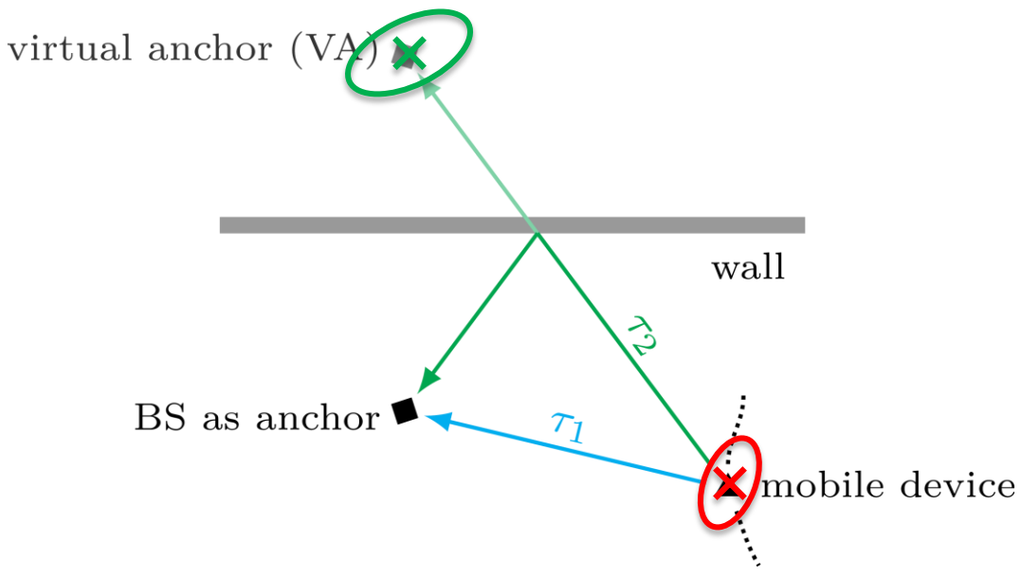

- **MP-SLAM:** Jointly estimates the mobile device position and the propagation environment by exploiting multipath propagation

- **Virtual anchors (VAs):** Model specular reflections via mirror images of physical anchors (PAs)

↓

Estimated VA positions act as additional PAs improving localization accuracy and robustness

MP-SLAM: Limitations of VAs

- For each PA one individual virtual anchor (VA) for each reflecting surface
- Multiple-bounce path-related VAs are related to more than one reflecting surface
- No data fusion between PAs and multiple-bounce reflections possible

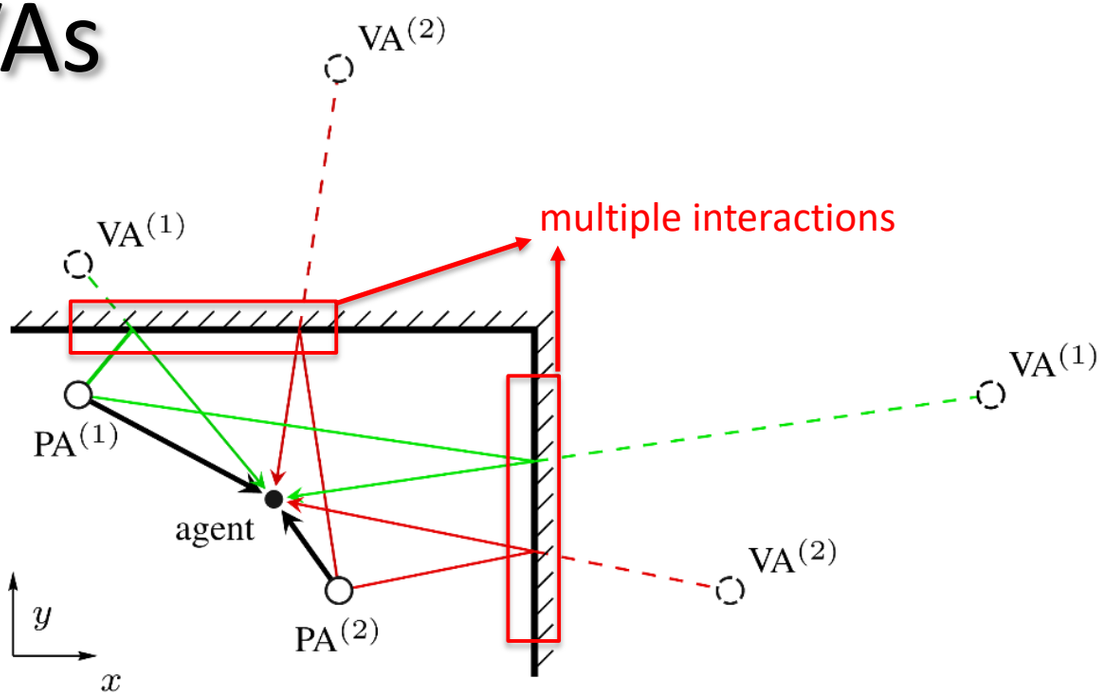

- Multiple measurements of same map feature!
- VA model: does not consistently combine measurements related to same map features
- Data fusion with surface feature vectors (SFVs)

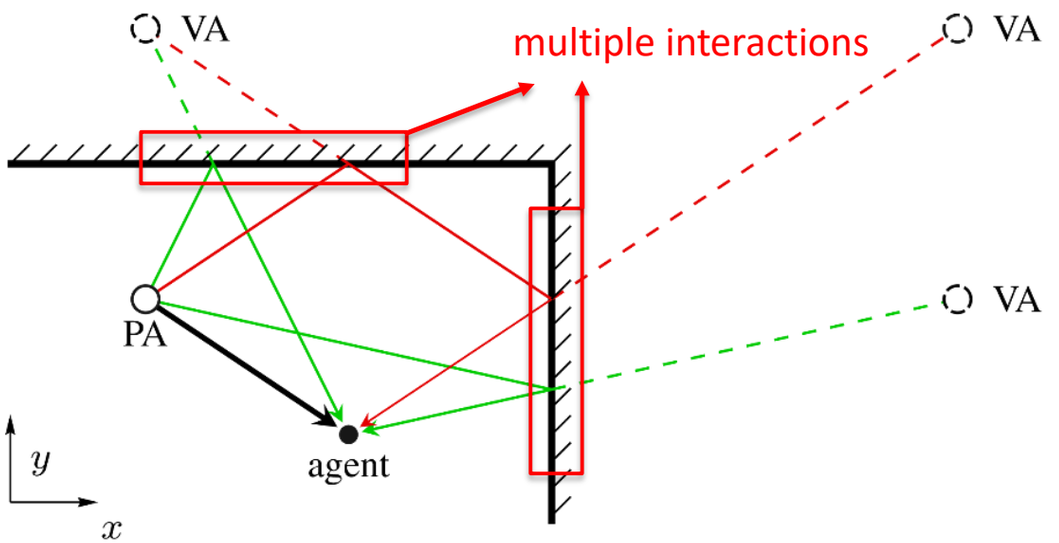

Surface Feature Vectors To Virtual Anchors

- **Multiple paths per surface:** A reflecting surface generates multiple propagation paths ⇒ multiple VAs

- **Surface feature vector (SFV)** concept: A SFV is the mirror image of the origin at each reflecting surface

- **Geometric relation:** SFV position $\mathbf{p}_{s,\mathrm{sfv}}$ maps to VA positions $\mathbf{p}_{ss,\mathrm{va}}^{(j)}$ given PA position $\mathbf{p}_{\mathrm{pa}}^{(j)}$

$$\boldsymbol{p}_{ss,\mathrm{va}}^{(j)} = \boldsymbol{p}_{\mathrm{pa}}^{(j)} - \left(\frac{2 \boldsymbol{p}_{\mathrm{pa}}^{(j)\mathsf{T}} \boldsymbol{p}_{s,\mathrm{sfv}}}{\|\boldsymbol{p}_{s,\mathrm{sfv}}\|^2} - 1 \right) \boldsymbol{p}_{s,\mathrm{sfv}}$$

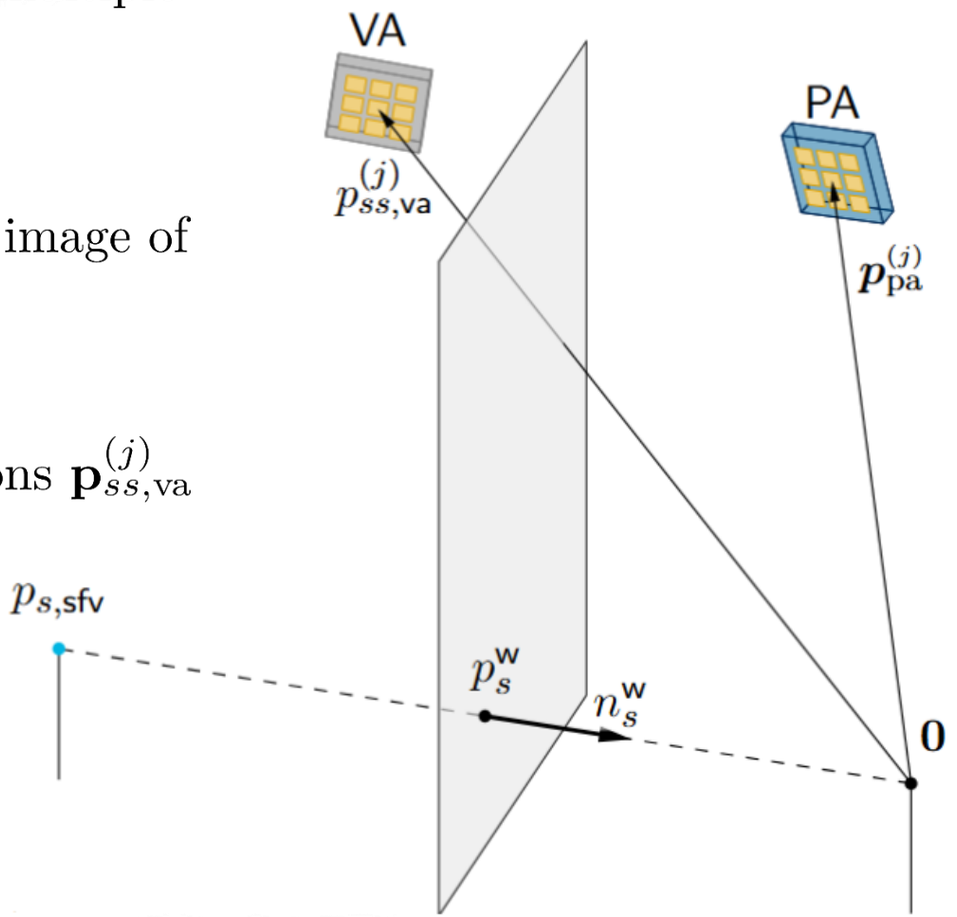

SFV links VAs of the same surface ⇒ data fusion across PAs and multiple-bounce paths

Surface Feature Vectors To Virtual Anchors

- **Global** cartesian coordinates PA j:

$$\boldsymbol{r}_{s,n}^{(j)} = \boldsymbol{p}_n - \boldsymbol{p}_{ss,\mathrm{va}}^{(j)} \quad \ldots \quad \text{VA} \rightarrow \text{agent}$$

$$\widetilde{\boldsymbol{r}}_{s,n}^{(j)} = \left(\boldsymbol{I}_3 - 2\frac{\boldsymbol{p}_{s,\mathrm{sfv}}\boldsymbol{p}_{s,\mathrm{sfv}}^{\mathsf{T}}}{\|\boldsymbol{p}_{s,\mathrm{sfv}}\|}\right)\boldsymbol{r}_{s,n}^{(j)} \quad \ldots \quad \text{PA} \rightarrow \text{virtual agent}$$

- **Local** cartesian coordinates PA j:

$$\acute{\boldsymbol{r}}_{s,n}^{(j)} = \boldsymbol{M}_j^{-1}\widetilde{\boldsymbol{r}}_{s,n}^{(j)}(\boldsymbol{p}_n, \boldsymbol{p}_{s,\mathrm{sfv}}) \quad \ldots \quad \text{PA} \rightarrow \text{virtual agent}$$

$$\boldsymbol{M}_j \in SO(3) \subset \mathbb{R}^{3\times 3} \quad \ldots \quad \text{rotation matrix of PA } j$$

- **Local** spherical coordinates PA j:

$$\tau_{s,n}^{(j)} = \frac{\|\acute{\boldsymbol{r}}_{s,n}^{(j)}\|}{\mathrm{c}}$$

$$\theta_{s,n}^{(j)} = \arccos\left([\acute{\boldsymbol{r}}_{s,n}^{(j)}]_3 / \|\acute{\boldsymbol{r}}_{s,n}^{(j)}\|\right)$$

$$\vartheta_{s,n}^{(j)} = \mathrm{atan2}\left([\acute{\boldsymbol{r}}_{s,n}^{(j)}]_2, [\acute{\boldsymbol{r}}_{s,n}^{(j)}]_1\right)$$

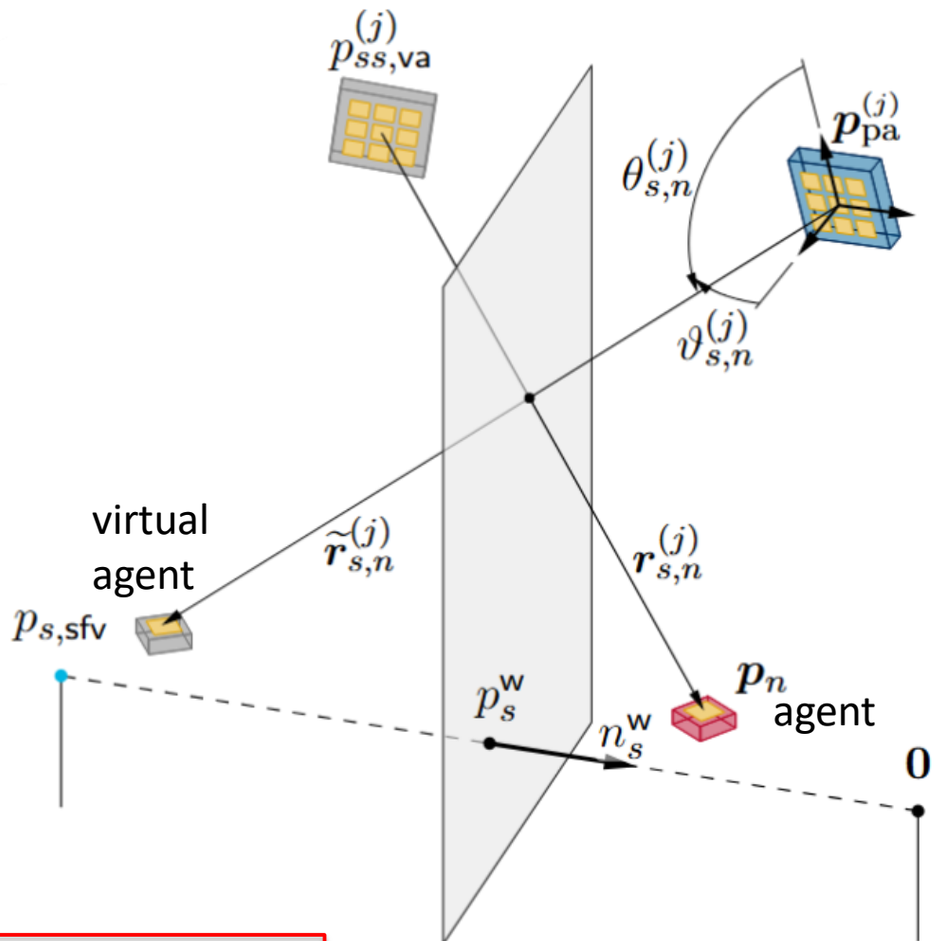

⇒ Parameters $\boldsymbol{\theta}_{s,n}^{(j)}$ are a function of agent position $\boldsymbol{p}_n$ and SFV positions $\boldsymbol{p}_{s,\mathrm{sfv}}$

⇒ Local array: planar wavefront approximation → global D-MIMO/XL-MIMO: ⇒ spherical wavefront

Radio Signal Model

Received radio signal at time n and PA j (BS, sub-array, distributed array):

$$\boldsymbol{z}_n^{(j)} = \sum_{k=0}^{K} \rho_{k,n}^{(j)} \boldsymbol{\psi}_k(\boldsymbol{\theta}_{k,n}^{(j)}) + \boldsymbol{w}_n^{(j)}$$

- $\rho_{k,n}^{(j)} \in \mathbb{C}$ complex amplitude of MPC k
- $\boldsymbol{\theta}_{k,n}^{(j)} = \left[\tau_{k,n}^{(j)} \;\; \theta_{k,n}^{(j)} \;\; \vartheta_{k,n}^{(j)}\right]^{\mathrm{T}}$

  $\tau_{k,n}^{(j)}$ delay of MPC $k \longleftrightarrow \frac{\|\acute{\boldsymbol{r}}_{s,n}^{(j)}\|}{\mathrm{c}}$

  $\theta_{k,n}^{(j)}$ elevation of MPC $k \longleftrightarrow \arccos\left([\acute{\boldsymbol{r}}_{s,n}^{(j)}]_3 / \|\acute{\boldsymbol{r}}_{s,n}^{(j)}\|\right)$

  $\vartheta_{k,n}^{(j)}$ azimuth of MPC $k \longleftrightarrow \mathrm{atan2}\left([\acute{\boldsymbol{r}}_{s,n}^{(j)}]_2, [\acute{\boldsymbol{r}}_{s,n}^{(j)}]_1\right)$

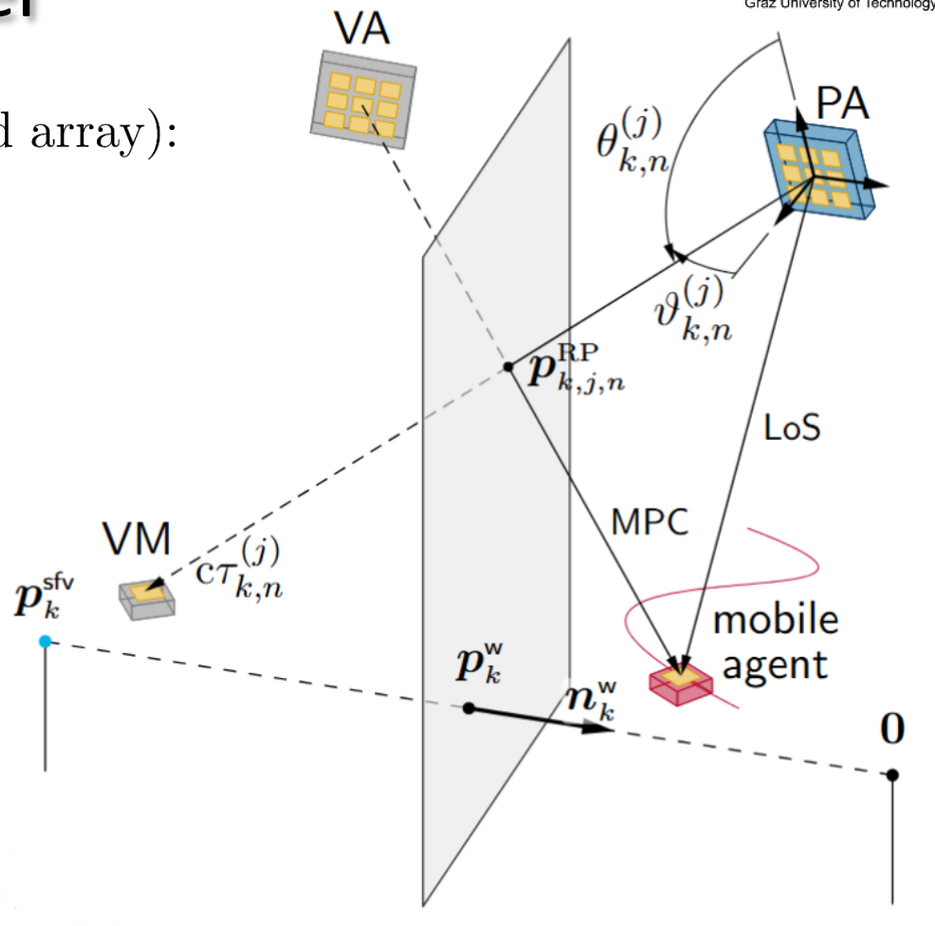

- Array vectors $\boldsymbol{\psi}(\boldsymbol{\theta}) = \frac{\lambda_\mathrm{c}}{4\pi\tau} S(\mathbf{f}) \odot \left(\exp(\mathrm{j}2\pi\mathbf{f}\tau) \otimes \boldsymbol{a}(\theta,\vartheta)\right) \exp(-\mathrm{j}2\pi f_\mathrm{c}\tau) \;\in \mathbb{C}^{N_\mathrm{f} M}$
- Noise described by covariance matrix $\boldsymbol{C}_{\mathrm{w},n}^{(j)}$

Two-Step Approach versus Direct Approach

Two-step Approaches

- Detection and estimation of MPC parameters using the radio signal

  → Estimated MPC parameters $\hat{\theta}$:
  - Subspace methods (e.g. Tensor-ESPRIT)
  - orthogonal matching pursuit (OMP)
  - Newtonized OMP (NOMP)
  - RiMAX
  - sparse Bayesian learning (SBL)
  - SBL with dictionary learning (SBLD)

- Graph-based inference with MPC parameters

  → data association (DA): assignment between MPCs and map features/objects

Direct Approaches (later)

- Graph-based inference using raw radio signal

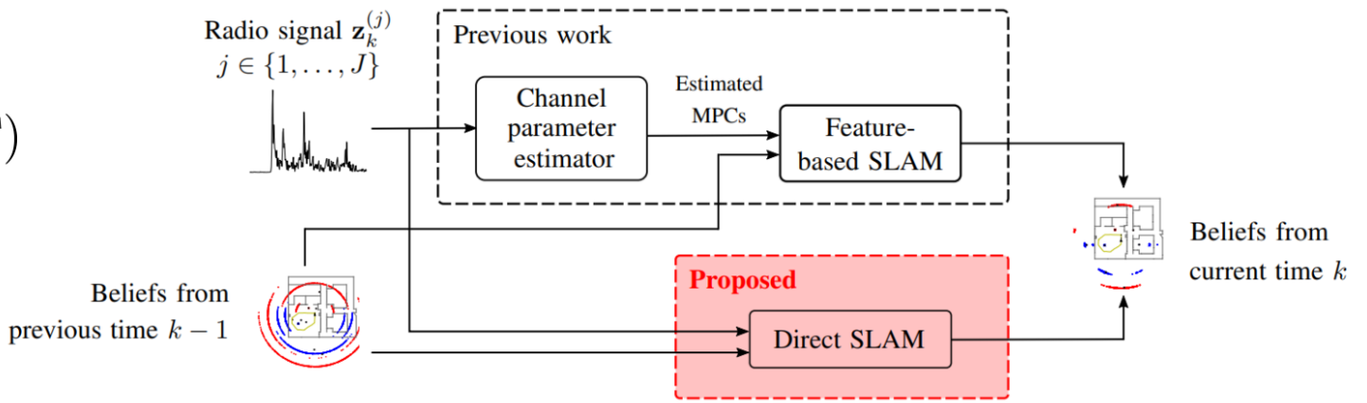

- Graph-based inference using raw radio signal

  → no DA: implicit probabilistic assignment

Two-Step Approach: Signal Parameter Estimation

- Multi-dimensional **multipath parameters**: $\boldsymbol{y} = \sum_{k=1}^{K} \rho_k \boldsymbol{\psi}_k(\boldsymbol{\theta}_k) + \boldsymbol{v}(\boldsymbol{\eta})$

- **Fast sparse Bayesian learning with dictionary estimation**
  - Number of MPCs via estimation of sparsity-inducing hyperparameters $\hat{\boldsymbol{\gamma}}$ (plus detection threshold $\rightarrow$ false positive control)
  - Dictionary estimation $\rightarrow \hat{\boldsymbol{\theta}}$ (Resolving of closely spaced SMCs)
  - Estimation of noise power and statistical multipath parameters $\hat{\boldsymbol{\eta}}$
  - Posterior PDF of complex amplitudes ρ_k estimated based on other parameters

Angular-delay spectrum of a radio signal**:**

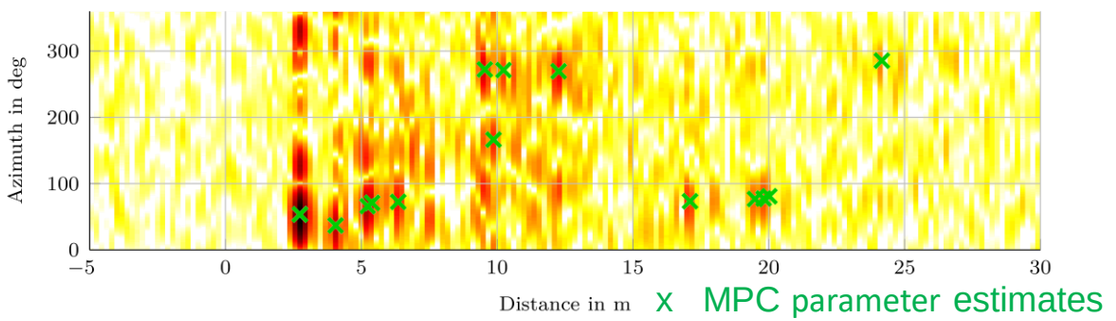

S. Grebien, E. Leitinger, K. Witrisal, and B. H. Fleury, “Super-resolution estimation of UWB channels including the dense component – An SBL-inspired approach,” IEEE Trans. Wireless Commun., 2024.
J. Möderl, E. Leitinger, F. Pernkopf, K. Witrisal, “Variational inference of structured line spectra exploiting group-sparsity,” IEEE Trans. Signal Process, 2024.
J. Möderl, E. Leitinger, B. H. Fleury, F. Pernkopf, and K. Witrisal,“Fast variational block-sparse Bayesian learning,” IEEE Trans. SignalProcess., 2025.
J. Möderl, A. M. Westerkam, A. Venus, and E. Leitinger, “A block-sparse Bayesian learning algorithm with dictionary parameter estimation for multi-sensor data fusion,” in Proc. Fusion-2025, Brasil, Rio De Janeiro,Jul. 2025.

Two-Step Approach: Signal Parameter Estimation

- Multi-dimensional **multipath parameters**: $\boldsymbol{y} = \sum_{k=1}^{K} \rho_k \boldsymbol{\psi}_k(\boldsymbol{\theta}_k) + \boldsymbol{v}(\boldsymbol{\eta})$

- **Fast sparse Bayesian learning with dictionary estimation**
  - Number of MPCs via estimation of sparsity-inducing hyperparameters $\hat{\boldsymbol{\gamma}}$ (plus detection threshold $\rightarrow$ false positive control)
  - Dictionary estimation $\rightarrow \hat{\boldsymbol{\theta}}$ (Resolving of closely spaced SMCs)
  - Estimation of noise power and statistical multipath parameters $\hat{\boldsymbol{\eta}}$
  - Posterior PDF of complex amplitudes ρ_k estimated based on other parameters

Angular-delay spectrum of a radio signal**:**

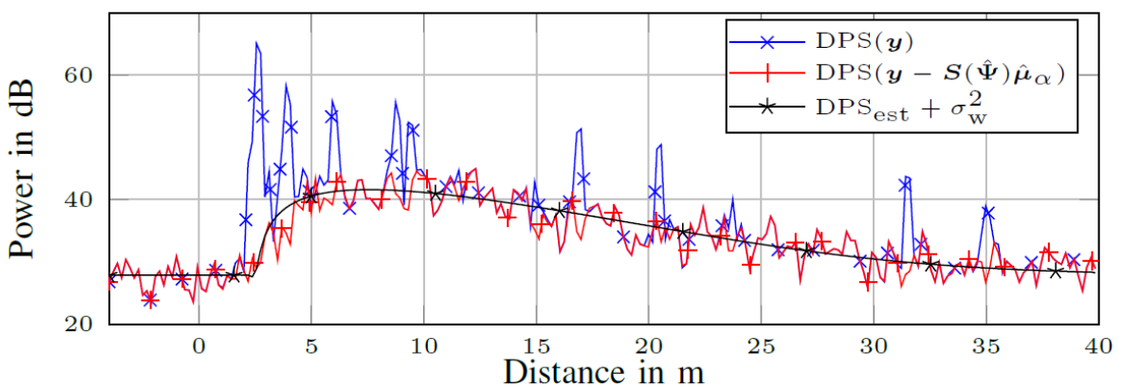

S. Grebien, E. Leitinger, K. Witrisal, and B. H. Fleury, "Super-resolution estimation of UWB channels including the dense component – An SBL-inspired approach," IEEE Trans. Wireless Commun., 2024.
J. Möderl, E. Leitinger, F. Pernkopf, K. Witrisal, "Variational inference of structured line spectra exploiting group-sparsity," IEEE Trans. Signal Process, 2024.
J. Möderl, E. Leitinger, B. H. Fleury, F. Pernkopf, and K. Witrisal,"Fast variational block-sparse Bayesian learning," IEEE Trans. SignalProcess., 2025.
J. Möderl, A. M. Westerkam, A. Venus, and E. Leitinger, "A block-sparse Bayesian learning algorithm with dictionary parameter estimation for multi-sensor data fusion," in Proc. Fusion-2025, Brasil, Rio De Janeiro,Jul. 2025.

Two-Step Approach: Signal Parameter Estimation

- Multi-dimensional **multipath parameters**: $\boldsymbol{y} = \sum_{k=1}^{K} \rho_k \boldsymbol{\psi}_k(\boldsymbol{\theta}_k) + \boldsymbol{v}(\boldsymbol{\eta})$

- **Fast sparse Bayesian learning with dictionary estimation**
  - Number of MPCs via estimation of sparsity-inducing hyperparameters $\hat{\boldsymbol{\gamma}}$ (plus detection threshold $\rightarrow$ false positive control)
  - Dictionary estimation $\rightarrow \hat{\boldsymbol{\theta}}$ (Resolving of closely spaced SMCs)
  - Estimation of noise power and statistical multipath parameters $\hat{\boldsymbol{\eta}}$
  - Posterior PDF of complex amplitudes ρ_k estimated based on other parameters

Angular-delay spectrum of a radio signal**:**

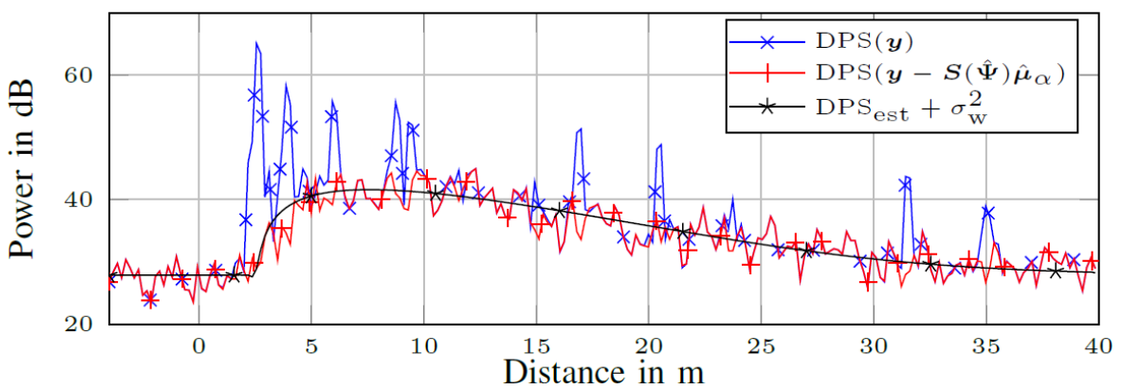

Resolving two crossing components:

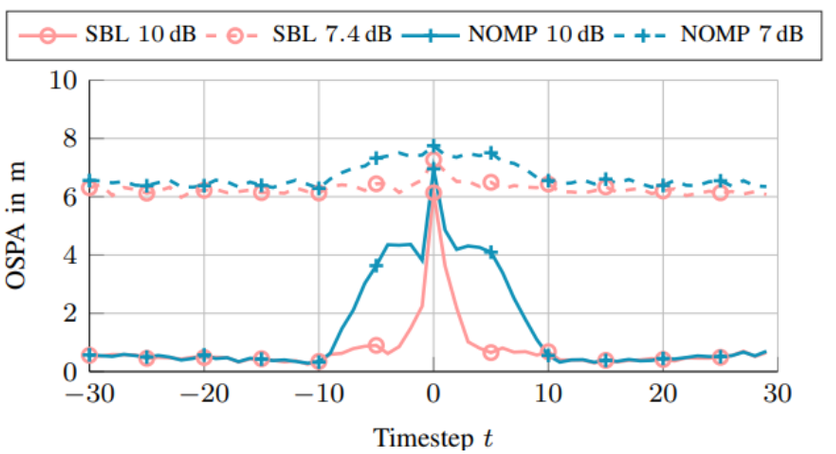

S. Grebien, E. Leitinger, K. Witrisal, and B. H. Fleury, "Super-resolution estimation of UWB channels including the dense component – An SBL-inspired approach," IEEE Trans. Wireless Commun., 2024.
J. Möderl, E. Leitinger, F. Pernkopf, K. Witrisal, "Variational inference of structured line spectra exploiting group-sparsity," IEEE Trans. Signal Process, 2024.
J. Möderl, E. Leitinger, B. H. Fleury, F. Pernkopf, and K. Witrisal,"Fast variational block-sparse Bayesian learning," IEEE Trans. SignalProcess., 2025.
J. Möderl, A. M. Westerkam, A. Venus, and E. Leitinger, "A block-sparse Bayesian learning algorithm with dictionary parameter estimation for multi-sensor data fusion," in Proc. Fusion-2025, Brasil, Rio De Janeiro,Jul. 2025.

Graph-based Inference

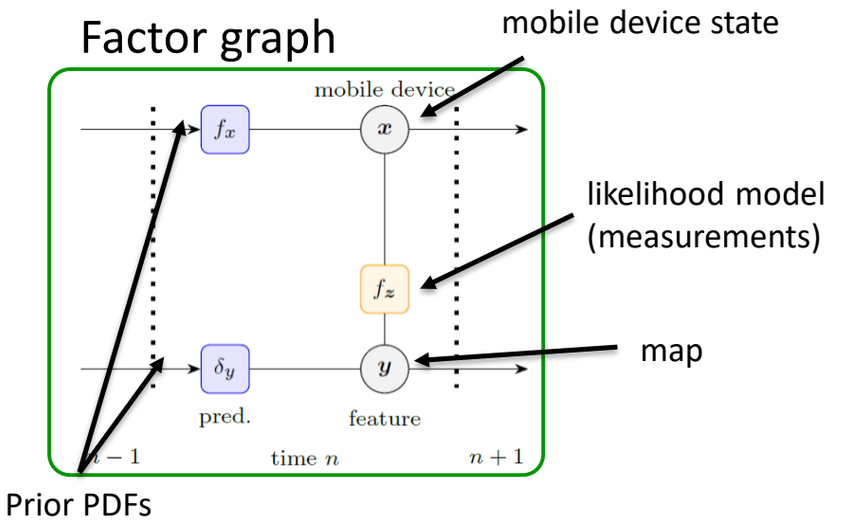

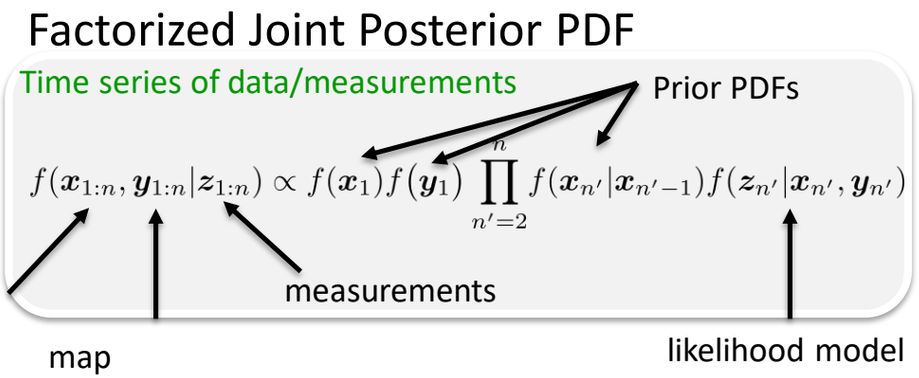

Issues:

- Little structure is exploited (only Markov property)
- High-dimensional random variables
- Algorithms are inefficient and scale not well with system parameters

- **Inference model parameters** described by a **joint posterior PDF**
- **Conditional independencies** are used to factorize the posterior PDF
- **Factor graph (FG)** encodes statistical relations in likelihood functions and prior PDFs
- **Efficient message passing methods** exploiting FG structure → estimation of the marginal posterior PDFs of parameters
- **"Natural" uncertainty quantification**

Scalable Graph-based Inference

Factor graph

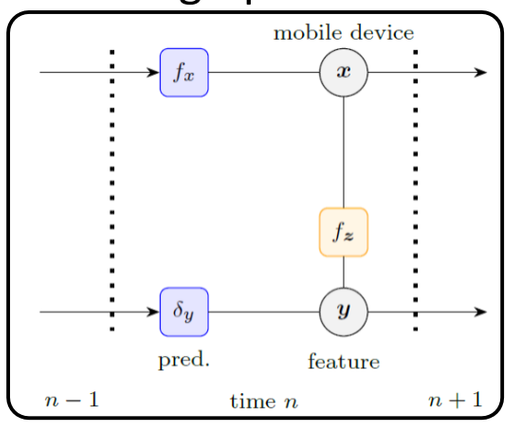

Independency assumptions between BS

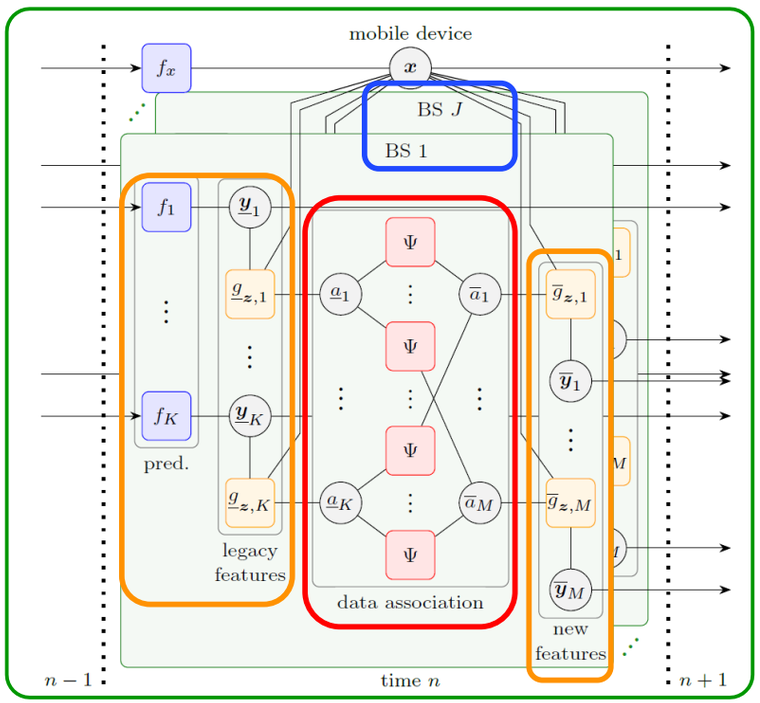

Independency assumptions between map features (VAs)

Loopy FG for data association

Factorized Joint Posterior PDF

Time series of data/measurements

$$f(\boldsymbol{x}_{1:n}, \boldsymbol{y}_{1:n}, \underline{\boldsymbol{a}}_{1:n}, \overline{\boldsymbol{a}}_{1:n} | \boldsymbol{z}_{1:n})$$

$$\propto f(\boldsymbol{x}_1) \left(\prod_{j'=1}^{J} \prod_{k'=1}^{K_1^{(j')}} f(\boldsymbol{y}_{k',1}^{(j')}) \right) \prod_{n'=2}^{n} f(\boldsymbol{x}_{n'} | \boldsymbol{x}_{n'-1})$$

$$\times \prod_{j=1}^{J} \left(\prod_{k=1}^{K_{n'-1}^{(j)}} f(\underline{\boldsymbol{y}}_{k,n'}^{(j)} | \boldsymbol{y}_{k,n'-1}^{(j)}) g(\boldsymbol{x}_{n'}, \underline{\boldsymbol{y}}_{k,n'}^{(j)}, \underline{a}_{k,n'}^{(j)}; \boldsymbol{z}_{n'}^{(j)}) \right.$$

$$\left. \times \prod_{m'=1}^{M_{n'}^{(j)}} \Psi_{km'}(\underline{a}_{k,n'}^{(j)}, \overline{a}_{m',n'}^{(j)}) \right)$$

$$\times \prod_{m=1}^{M_{n'}^{(j)}} f(\overline{\boldsymbol{y}}_{m,n}^{(j)} | \boldsymbol{x}_{n'}) h(\boldsymbol{x}_{n'}, \overline{\boldsymbol{y}}_{m,n'}^{(j)}, \overline{a}_{m,n'}^{(j)}; \boldsymbol{z}_{n'}^{(j)})$$

Solution:

- **Introduction of additional structure**: physical and statistical knowledge
- "Stretching" and "opening" FG nodes: **high-dimensional (non-linear) → lower-dimensional**
  - Scalable and efficient algorithms

Graphical Models in Diverse Applications

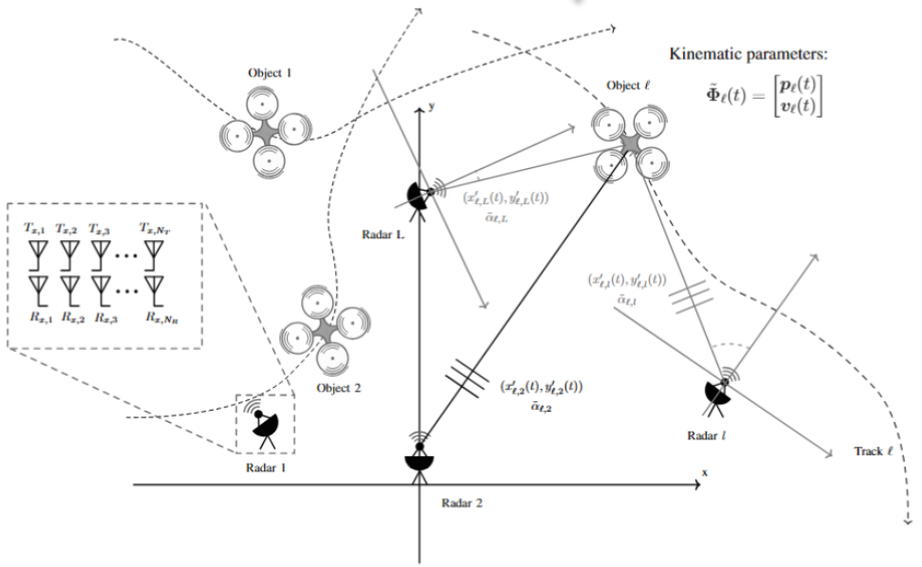

Multi-static MIMO Radar: MOT estimation, and tracking using **sparse Bayesian learning**, and **variational message passing**

A. M. Westerkam, J. Möderl, E. Leitinger, T. Pedersen, "A Variational Message Passing Framework for Multi-Sensor Multi-Object Tracking using Raw Radar Signals," arXiv, 2026.

J. Möderl, A. M. Westerkam, A. Venus and E. Leitinger, "A Block-Sparse Bayesian Learning Algorithm with Dictionary Parameter Estimation for Multi-Sensor Data Fusion," Proc. Fusion 2025, Rio de Janeiro, Brazil, 2025, pp. 1-8, doi: 10.23919/FUSION65864.2025.11124160.

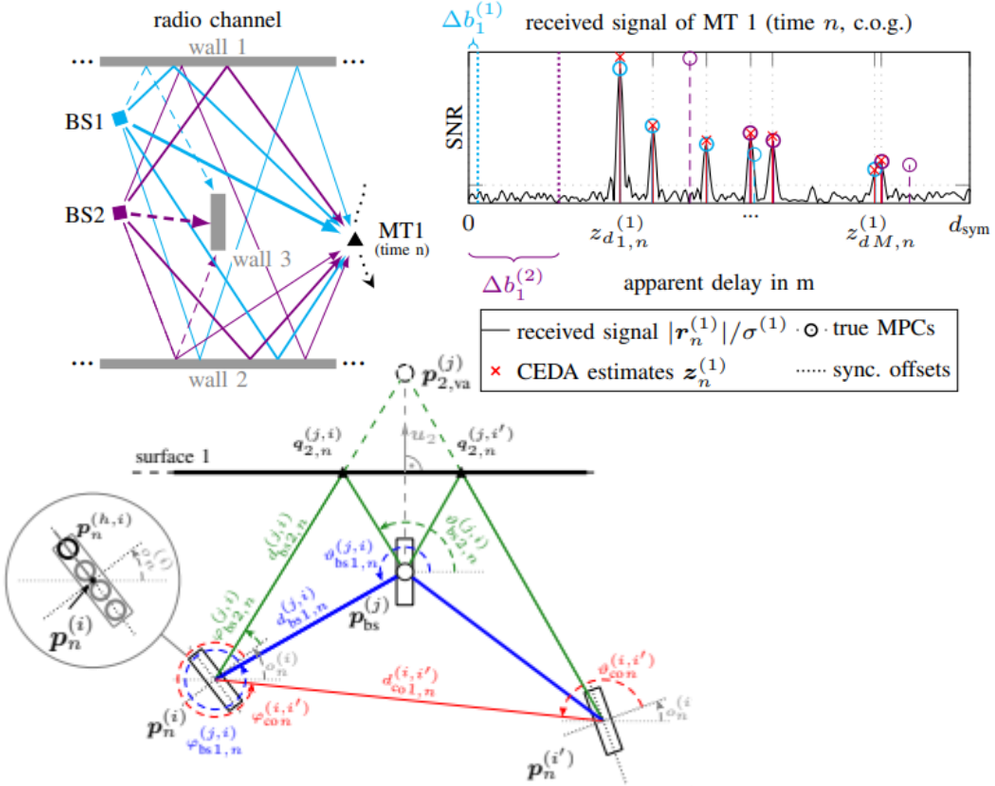

Cooperative MP-SLAM and Simultaneous Source Separation, Synchronization, Localization and Mapping using **factor graphs and belief propagation**

E. Leitinger, L. Wielandner, A. Venus, M. Liang, F. Meyer and K. Witrisal, "Multipath-Based SLAM with Cooperation and Map Fusion in MIMO Systems," Asilomar-2024, Pacific Grove, CA, USA, 2024, pp. 1316-1322, doi: 10.1109/IEEECONF60004.2024.10942778.

A. Venus, E. Leitinger, K. Witrisal, "Simultaneous Source Separation, Synchronization, Localization and Mapping for 6G Systems," arXiv, 2026.

Graphical Models in Diverse Applications

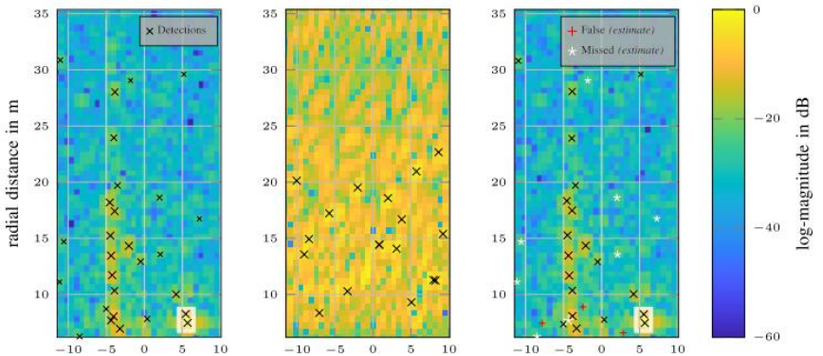

Variational signal separation for automotive radar Interference mitigation and MO inference using **sparse Bayesian learning** and **variational message passing**

M. Toth, E. Leitinger and K. Witrisal, "Variational Signal Separation for Automotive Radar Interference Mitigation," in IEEE Transactions on Radar Systems, vol. 2, pp. 1007-1026, 2024, doi: 10.1109/TRS.2024.3477353

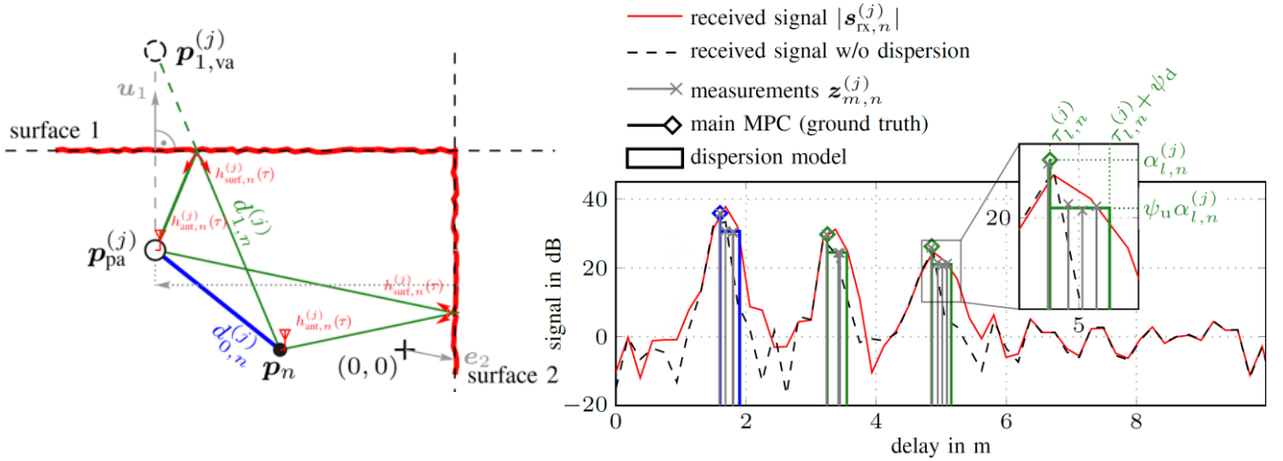

Multiple-measurement SLAM for rough surfaces and extended objects using **factor graphs and belief propagation**

L. Wielandner, A. Venus, T. Wilding, and E. Leitinger, “Multipath-based SLAM for non-ideal reflective surfaces exploiting multiple-measurement data association,” J. Adv. Inf. Fusion, vol. 18, pp. 59–77, Dec. 2023.

L. Wielandner, A. Venus, T. Wilding, K. Witrisal, and E. Leitinger, “MIMO multipath-based SLAM for non-ideal reflective surfaces,” in Proc. Fusion-2024, Venice, Italy, Jul. 2024.

Graphical Models for Bayesian Inference Applications

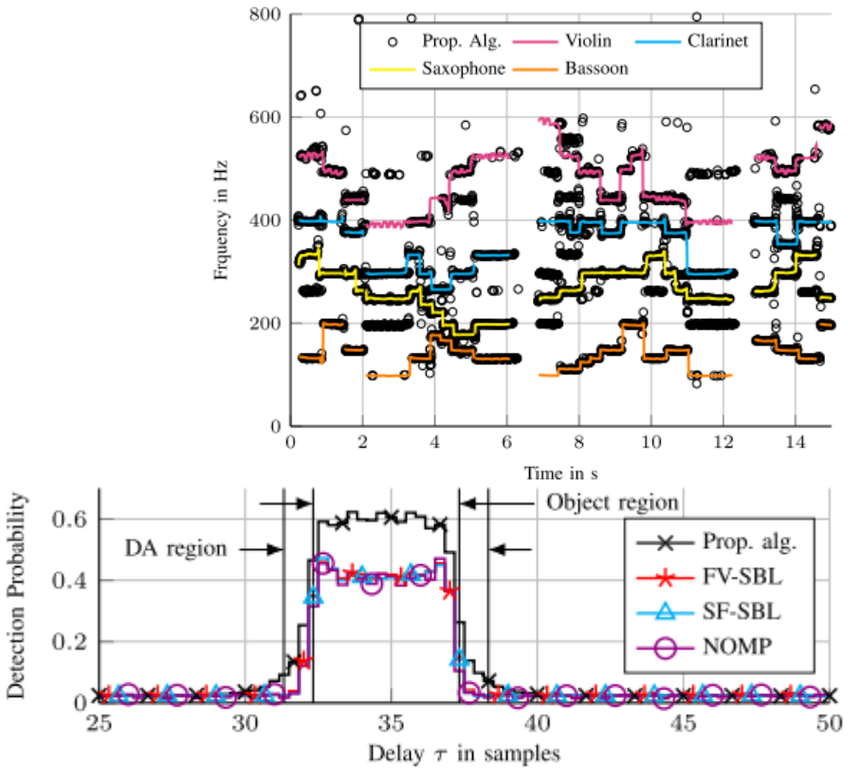

Multi-pitch tracking in music and extended object estimation using **variational inference exploiting hierarchical group sparsity**

J. Möderl, E. Leitinger, F. Pernkopf and K. Witrisal, "Variational Inference of Structured Line Spectra Exploiting Group-Sparsity," in IEEE Transactions on Signal Processing, vol. 74, pp. 499-513, 2026, doi: 10.1109/TSP.2024.3493603.

J. Möderl, E. Leitinger, B. H. Fleury, F. Pernkopf and K. Witrisal, "Fast Variational Block-Sparse Bayesian Learning," in IEEE Transactions on Signal Processing, vol. 73, pp. 4856-4872, 2025, doi: 10.1109/TSP.2025.3611234.

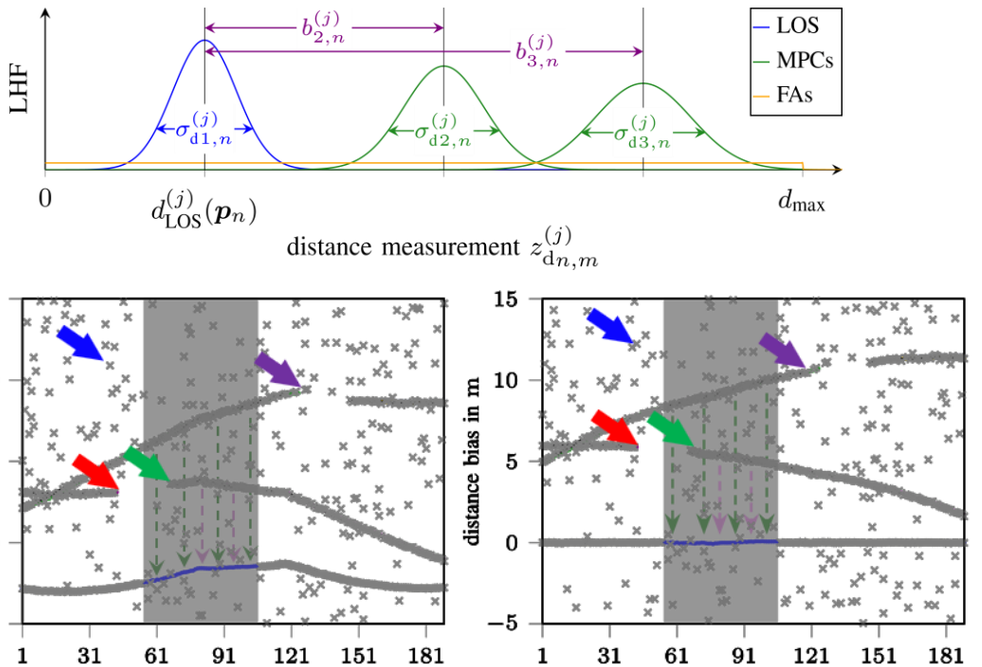

Simultaneous Localization and Bias Tracking using **factor graphs** and **belief propagation**

A. Venus, E. Leitinger, S. Tertinek, F. Meyer and K. Witrisal, "Graph-Based Simultaneous Localization and Bias Tracking," in IEEE Transactions on Wireless Communications, vol. 23, no. 10, pp. 13141-13158, Oct. 2024, doi: 10.1109/TWC.2024.3399023.

A. Venus, E. Leitinger, S. Tertinek and K. Witrisal, "A Graph-Based Algorithm for Robust Sequential Localization Exploiting Multipath for Obstructed-LOS-Bias Mitigation," in IEEE Transactions on Wireless Communications, vol. 23, no. 2, pp. 1068-1084, Feb. 2024, doi: 10.1109/TWC.2023.3285530.

Adaptive Multipath-based SLAM for D-MIMO

- **Agent:** $\mathbf{x}_n \triangleq \left[\mathbf{p}_n^\top \ \mathbf{v}_n^\top \ \Delta\varphi_n\right]^\top$

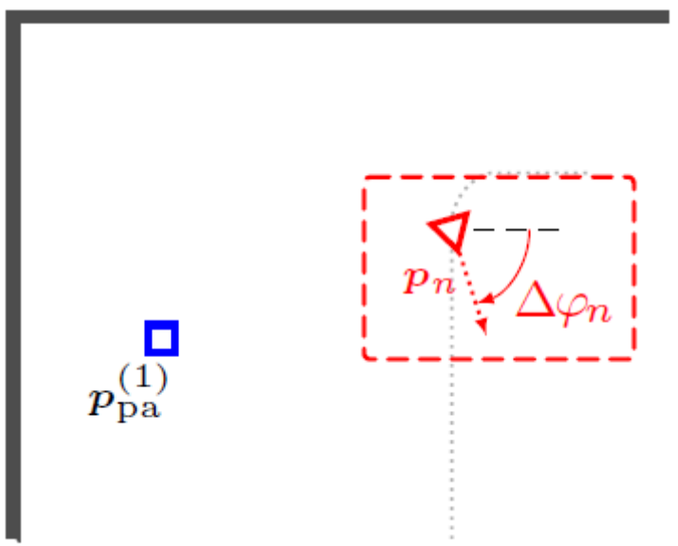

Adaptive Multipath-based SLAM for D-MIMO

- **Agent:** $\mathbf{x}_n \triangleq \left[\mathbf{p}_n^\top \ \mathbf{v}_n^\top \ \Delta\varphi_n\right]^\top$
- **Potential surface vector (SFV):** $\mathbf{y}_{s,n} \triangleq \left[\mathbf{p}_{s,\mathrm{sfv}}^\top \ r_{s,n}\right]^\top$
  - Binary existence variable: $r_{s,n} \in \{0, 1\}$
  - Legacy PSFVs $\mathbf{y}_{k,n}$ and new PSFVs $\mathbf{y}_{m,n}$

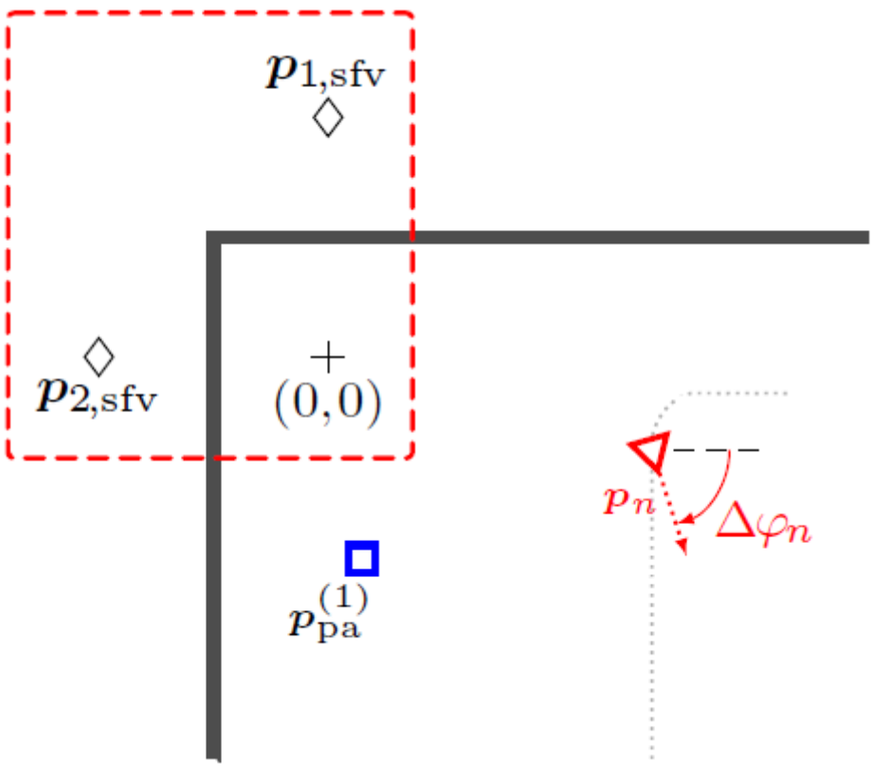

Adaptive Multipath-based SLAM for D-MIMO

- **Agent:** $\mathbf{x}_n \triangleq \left[\mathbf{p}_n^\top \; \mathbf{v}_n^\top \; \Delta\varphi_n\right]^\top$
- **Potential surface vector (SFV):** $\mathbf{y}_{s,n} \triangleq \left[\mathbf{p}_{s,\mathrm{sfv}}^\top \; r_{s,n}\right]^\top$
  - Binary existence variable: $r_{s,n} \in \{0, 1\}$
  - Legacy PSFVs $\mathbf{y}_{k,n}$ and new PSFVs $\mathbf{y}_{m,n}$

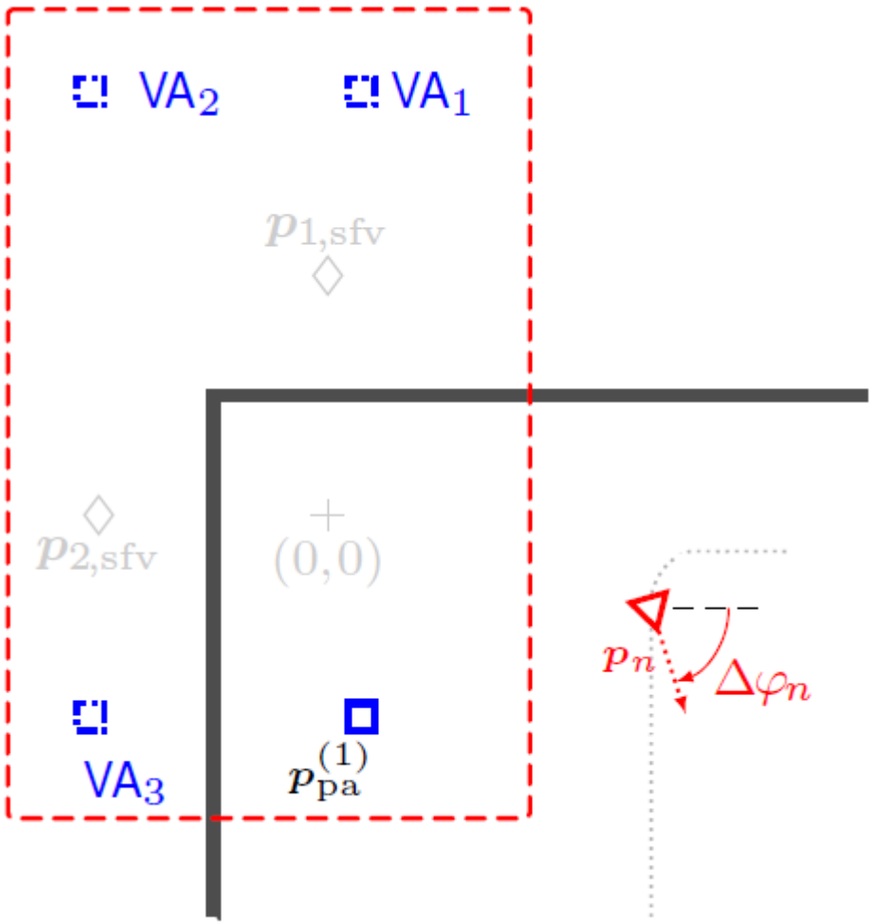

Adaptive Multipath-based SLAM for D-MIMO

- **Agent:** $\mathbf{x}_n \triangleq \left[\mathbf{p}_n^\top \; \mathbf{v}_n^\top \; \Delta\varphi_n\right]^\top$
- **Potential surface vector (SFV):** $\mathbf{y}_{s,n} \triangleq \left[\mathbf{p}_{s,\mathrm{sfv}}^\top \; r_{s,n}\right]^\top$
  - Binary existence variable: $r_{s,n} \in \{0,1\}$
  - Legacy PSFVs $\mathbf{y}_{k,n}$ and new PSFVs $\mathbf{y}_{m,n}$
- **Potential ray (PR):** $\boldsymbol{\beta}_{ss',n} \triangleq \left[u_{ss',n}^{(j)} \; r_{ss',n}^{(j)}\right]^\top$
  - Binary existence variable: $r_{ss',n}^{(j)} \in \{0,1\}$
  - Norm. amplitude: $u_{ss',n}^{(j)}$
  - $\Rightarrow$ measurement-related variance and $P_d\left(u_{ss',n}^{(j)}\right)$

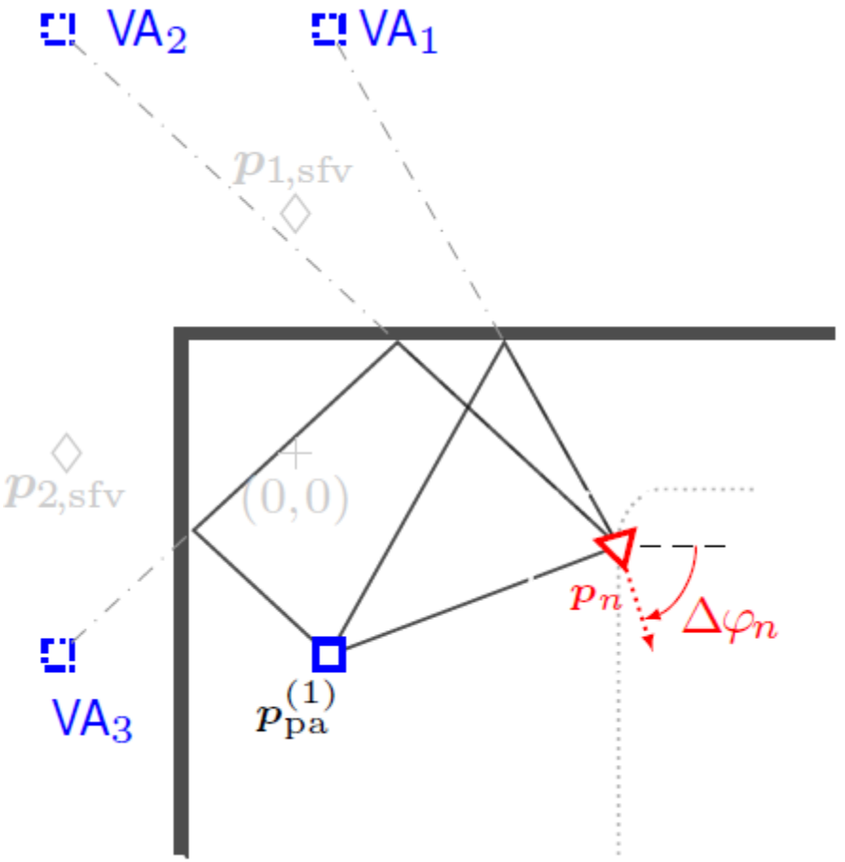

Adaptive Multipath-based SLAM for D-MIMO

- **Agent:** $\mathbf{x}_n \triangleq \left[\mathbf{p}_n^\top \; \mathbf{v}_n^\top \; \Delta\varphi_n\right]^\top$
- **Potential surface vector (SFV):** $\mathbf{y}_{s,n} \triangleq \left[\mathbf{p}_{s,\mathrm{sfv}}^\top \; r_{s,n}\right]^\top$
  - Binary existence variable: $r_{s,n} \in \{0,1\}$
  - Legacy PSFVs $\mathbf{y}_{k,n}$ and new PSFVs $\mathbf{y}_{m,n}$
- **Potential ray (PR):** $\boldsymbol{\beta}_{ss',n} \triangleq \left[u_{ss',n}^{(j)} \; r_{ss',n}^{(j)}\right]^\top$
  - Binary existence variable: $r_{ss',n}^{(j)} \in \{0,1\}$
  - Norm. amplitude: $u_{ss',n}^{(j)}$
  - $\Rightarrow$ measurement-related variance and $P_d\left(u_{ss',n}^{(j)}\right)$

Two layer existence model

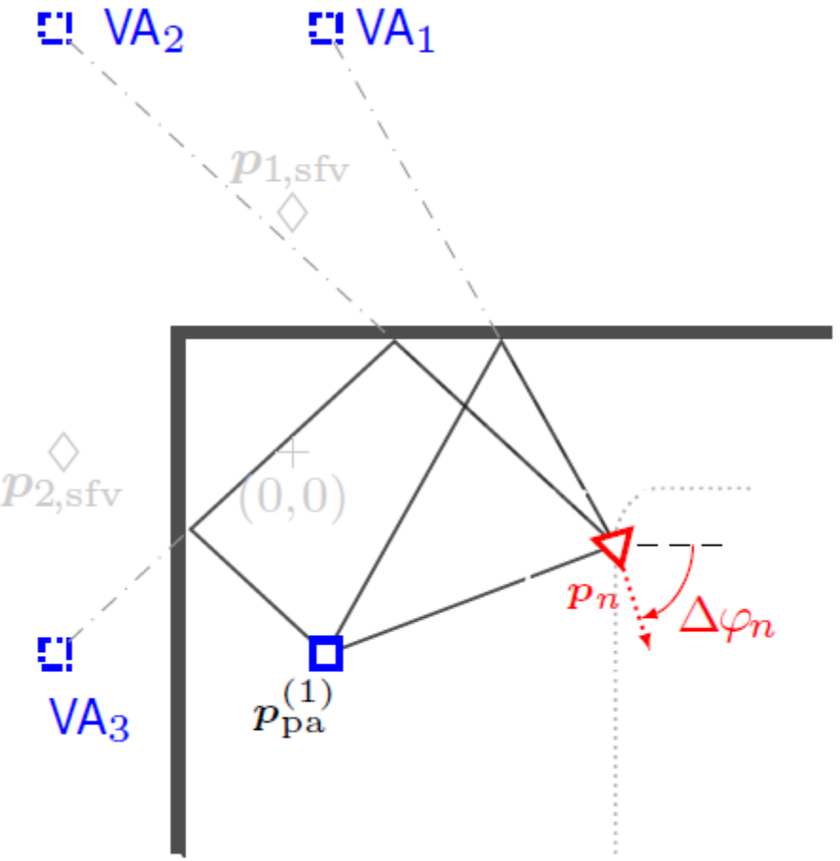

"soft" ray tracing

Adaptive Multipath-based SLAM for D-MIMO

- **Agent:** $\mathbf{x}_n \triangleq \left[\mathbf{p}_n^\top \ \mathbf{v}_n^\top \ \Delta\varphi_n\right]^\top$
- **Potential surface vector (SFV):** $\mathbf{y}_{s,n} \triangleq \left[\mathbf{p}_{s,\mathrm{sfv}}^\top \ r_{s,n}\right]^\top$
  - Binary existence variable: $r_{s,n} \in \{0,1\}$
  - Legacy PSFVs $\mathbf{y}_{k,n}$ and new PSFVs $\mathbf{y}_{m,n}$
- **Potential ray (PR):** $\boldsymbol{\beta}_{ss',n} \triangleq \left[u_{ss',n}^{(j)} \ r_{ss',n}^{(j)}\right]^\top$
  - Binary existence variable: $r_{ss',n}^{(j)} \in \{0,1\}$
  - Norm. amplitude: $u_{ss',n}^{(j)}$
  - $\Rightarrow$ measurement-related variance and $P_d\left(u_{ss',n}^{(j)}\right)$
- **Data association (DA) variables:** $\underline{a}_{s,n}^{(j)}$ and $\overline{a}_{m,n}^{(j)}$

Two layer existence model

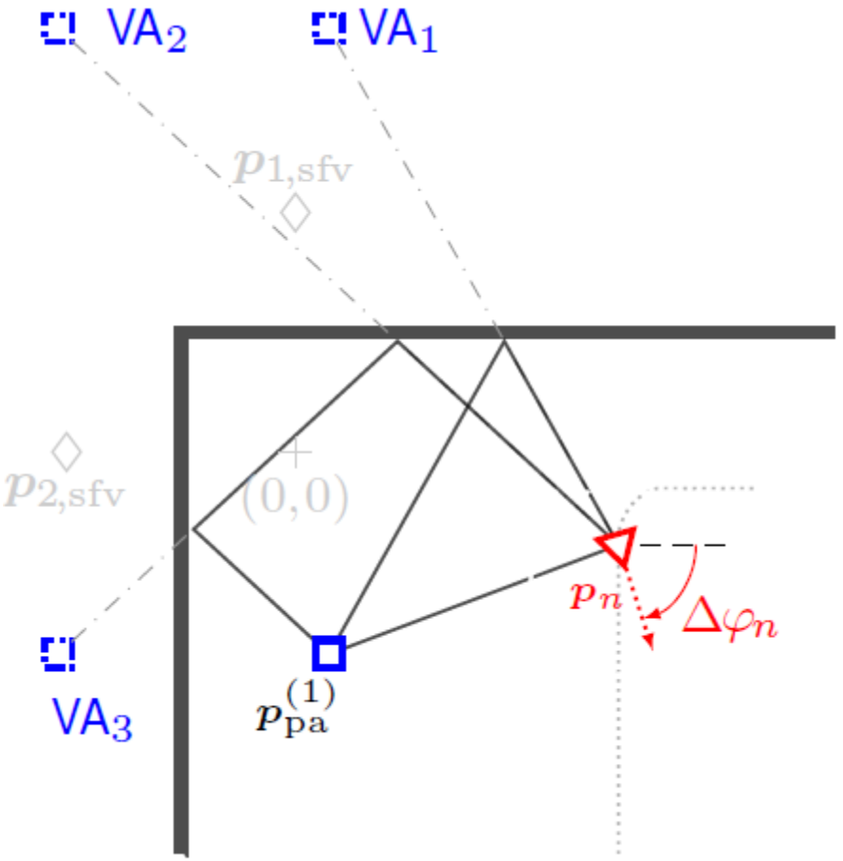

"soft" ray tracing

Adaptive Multipath-based SLAM for D-MIMO

Parametric channel estimator $\rightarrow$ Measurements at time n at jth PA:

- $\mathbf{z}_n^{(j)} \triangleq \left[\mathbf{z}_{1,n}^{(j)\top} \cdots \mathbf{z}_{M_n^{(j)},n}^{(j)\top}\right]^\top, \quad \mathbf{z}_{m,n}^{(j)} \triangleq \left[\hat{\tau}_{m,n}^{(j)}\ \hat{\varphi}_{m,n}^{(j)}\ \hat{\phi}_{m,n}^{(j)}\ \hat{u}_{m,n}^{(j)}\right]^\top$
- Normalized amplitude: $\hat{u}_{m,n}^{(j)} = \frac{|\hat{\alpha}_{m,n}^{(j)}|^2}{\hat{\sigma}^{(j)\,2}} \Rightarrow$ detection probability and adaptive measurement variance via Fisher information

Inference Problem

- Given: $\mathbf{z}_{1:n}^{(j)} \triangleq \left[\mathbf{z}_1^{(j)\mathrm{T}} \cdots \mathbf{z}_n^{(j)\mathrm{T}}\right]^\mathrm{T}$ with $j \in \{1, \ldots, J\}$
- Goal: Sequential detection and estimation of potential ray states and SFV states and estimation of agent state

E. Leitinger, A. Venus, B. Teague, and F. Meyer, "Data fusion for multipath-based SLAM: Combining information from multiple propagation paths," IEEE Trans. Signal Process.,2023.
X. Li, B. J. B. Deutschmann, E. Leitinger, and F. Meyer, "Adaptive multipath-based SLAM for distributed MIMO systems," IEEE Trans. Wireless Commun., 2026.

Joint Posterior PDF and Factor Graph

- Joint inference of agent state $\mathbf{x}_{0:n}$, PSFV states $\mathbf{y}_{0:n}$, PR states $\boldsymbol{\beta}_{0:n}$, DA variables $\underline{\mathbf{a}}_{1:n}$ and $\overline{\mathbf{a}}_{1:n}$
  - Joint posterior PDF: $f\left(\mathbf{x}_{0:n}, \mathbf{y}_{0:n}, \boldsymbol{\beta}_{0:n}, \underline{\mathbf{a}}_{1:n}, \overline{\mathbf{a}}_{1:n} | \mathbf{z}_{1:n}\right)$
  - Marginal posterior PDFs:

    $p(r_{s,n} = 1|\mathbf{z}_{1:n})$, $p(r^{(j)}_{ss',n} = 1|\mathbf{z}_{1:n})$, $f(\mathbf{p}_{s,\mathrm{sfv}}|r_{s,n} = 1, \mathbf{z}_{1:n})$, $f(\beta^{(j)}_{ss',n}|r^{(j)}_{ss',n} = 1, \mathbf{z}_{1:n})$, $f(\mathbf{x}_n|\mathbf{z}_{1:n})$

- Factorization of joint posterior PDF $\Rightarrow$ factor graph

$\rightarrow$ Message passing algorithm + particle-based implementation to approximate marginal PDFs

$\rightarrow$ MMSE estimation

Factor Graph

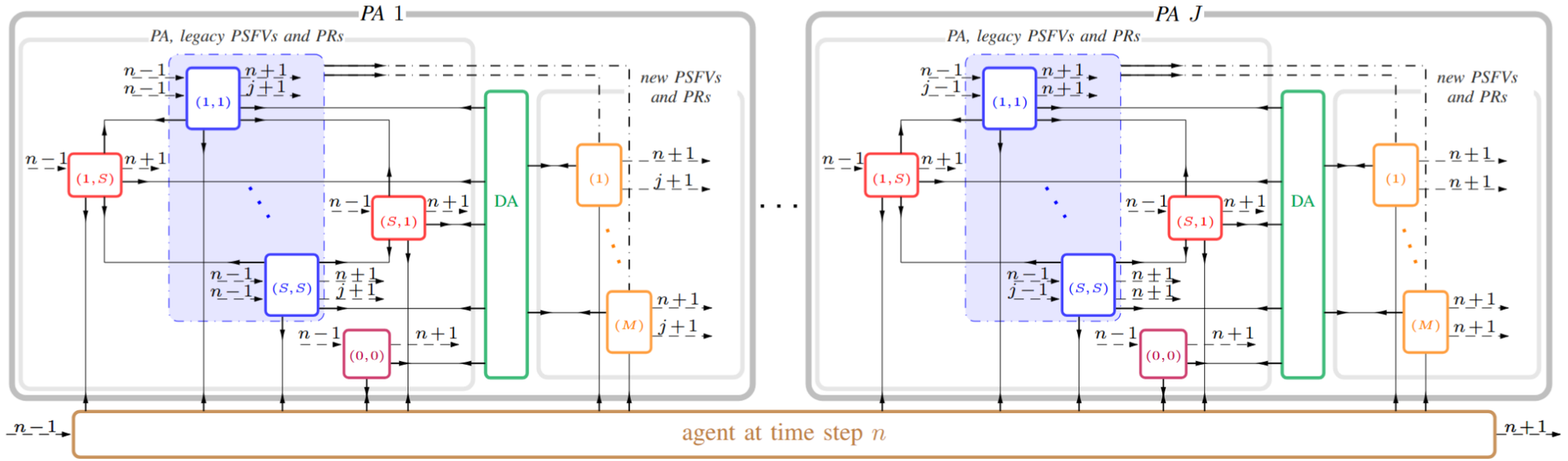

Agent + LOS path

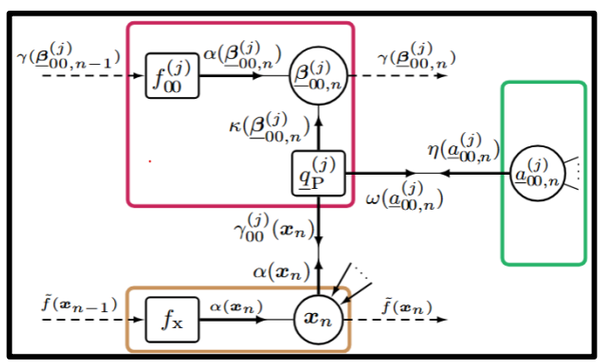

SFV and single-bounce path

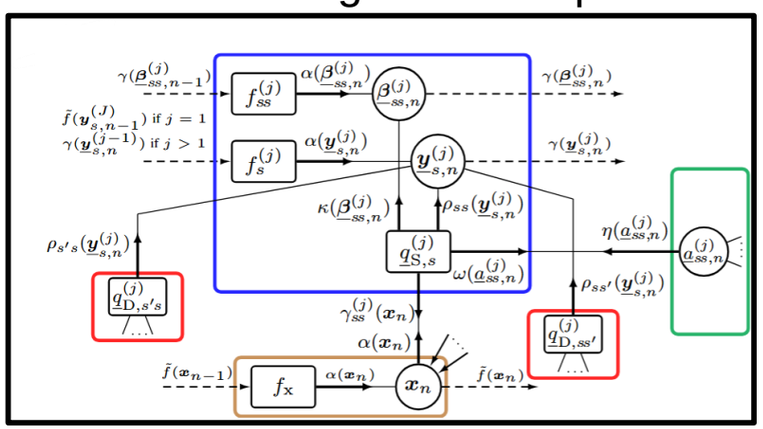

2 SFV and double-bounce path

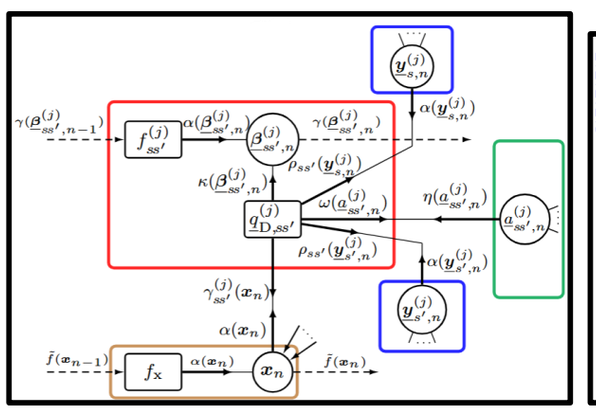

New SFVs and paths

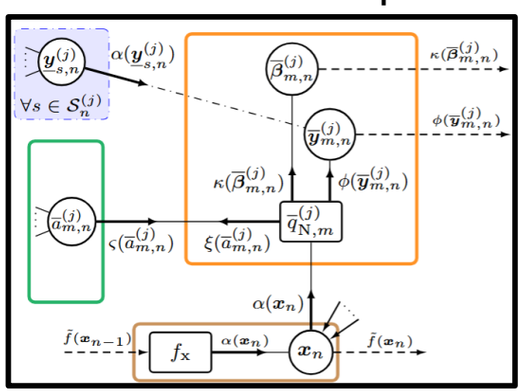

Measurement Results

- BW $= 100$ MHz
- $f_c = 6.25$ GHz
- 4 PAs: uniform array $(4 \times 4$-ele.$)$
- Agent: uniform array $(3 \times 3$-ele.$)$
- 40 snapshots

Measurement Results

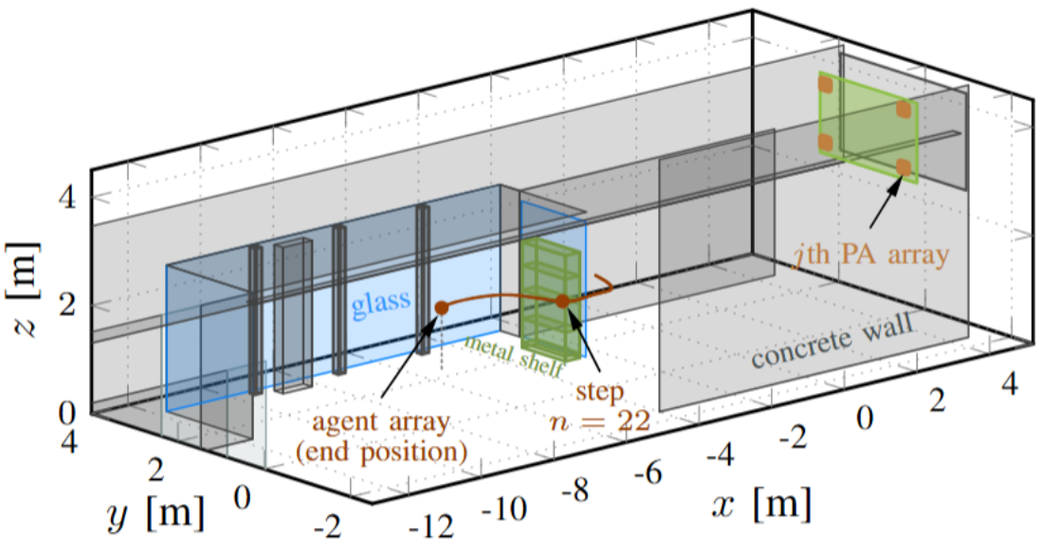

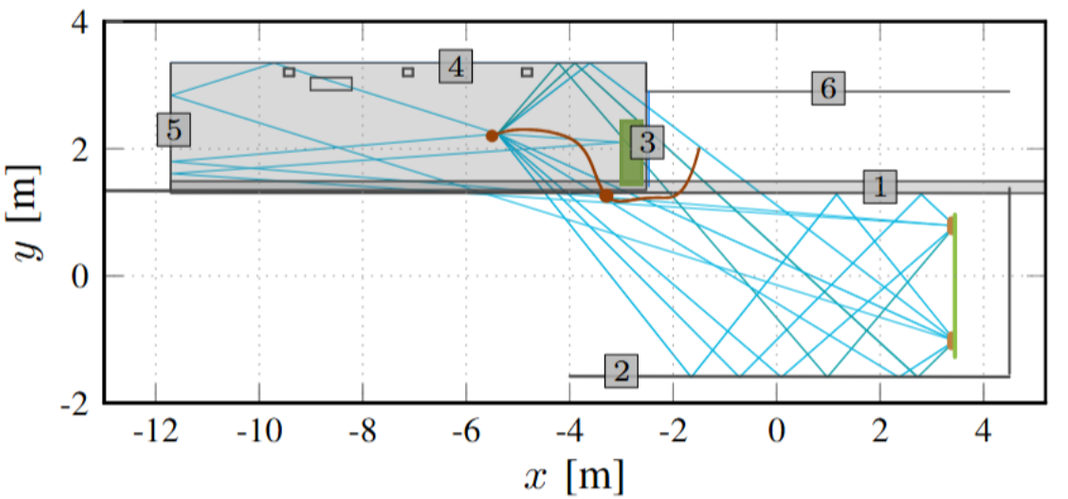

Measurement Results

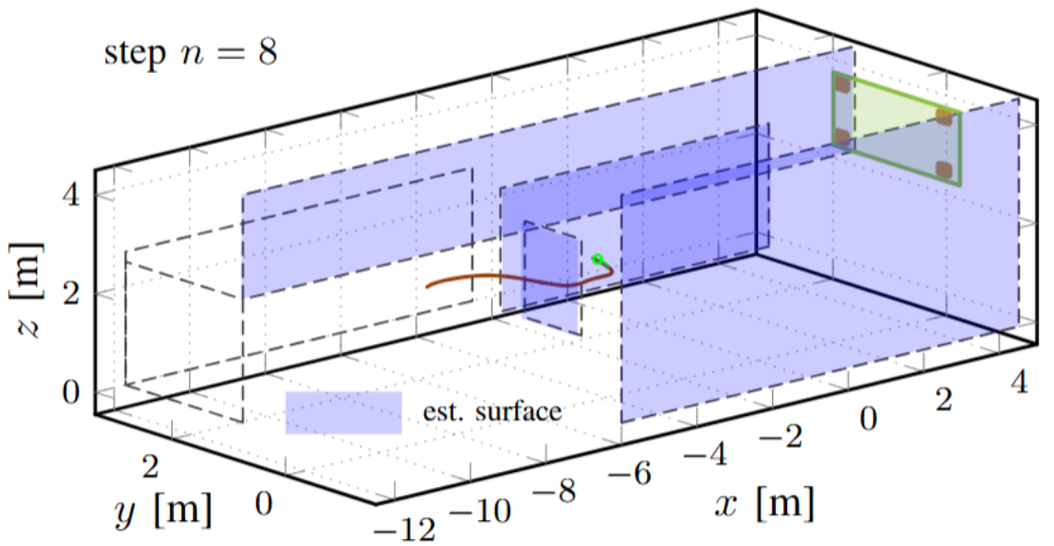

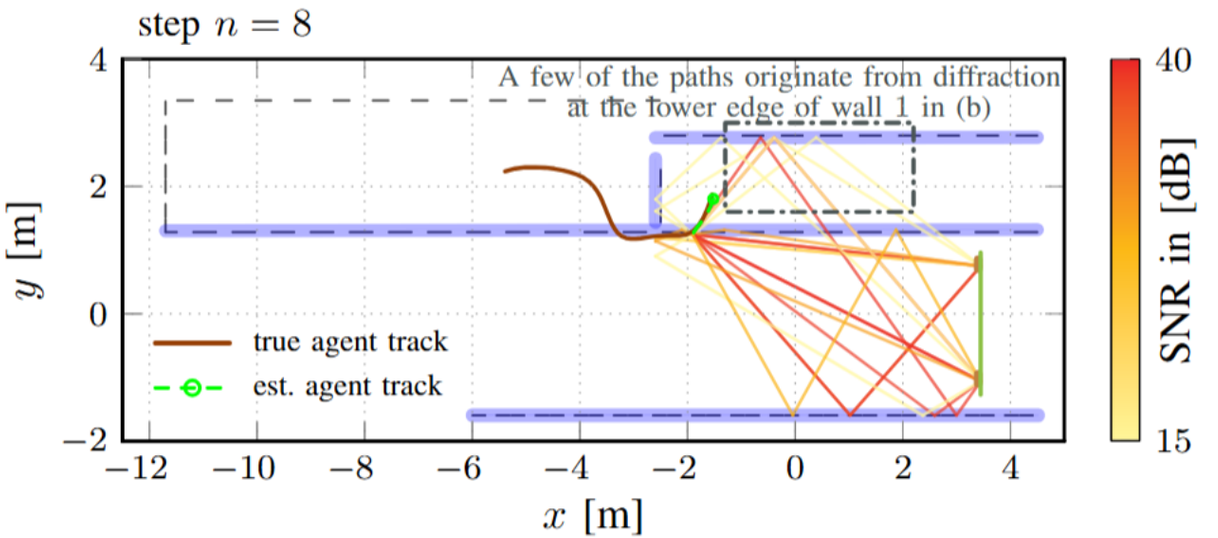

Agent RMSE

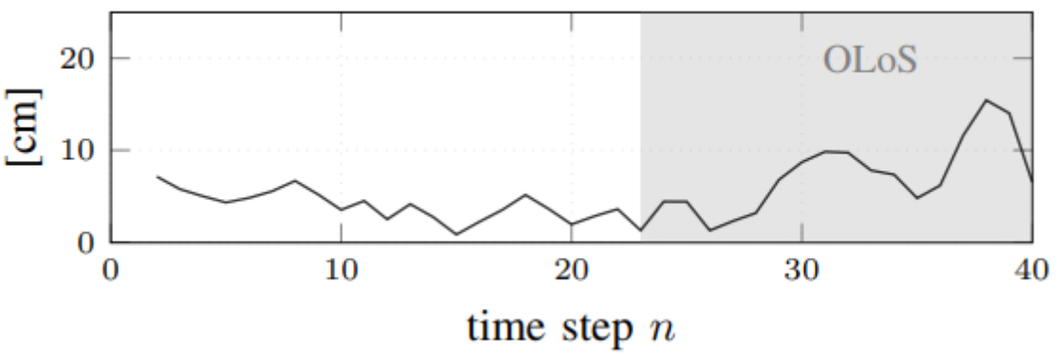

Measurement Results

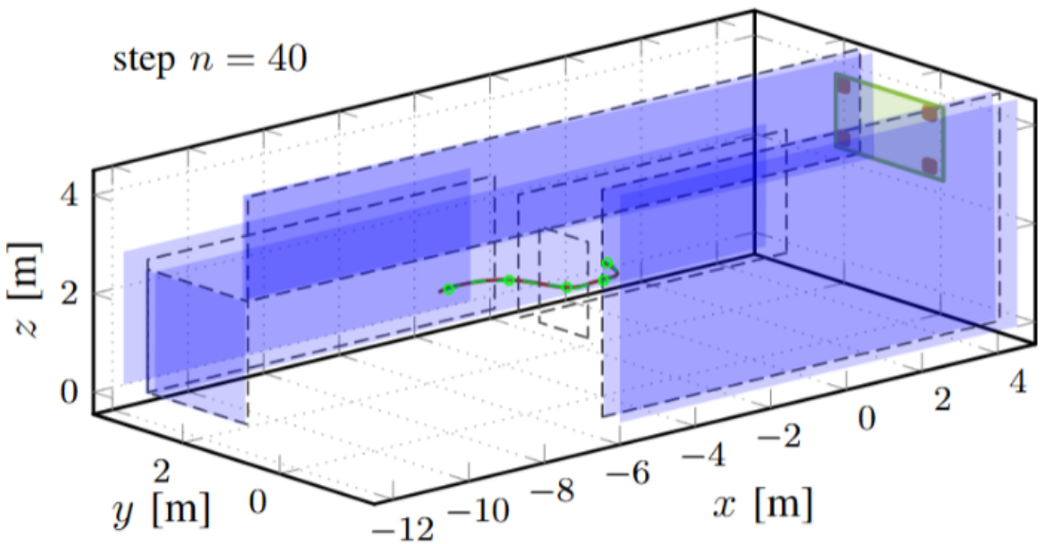

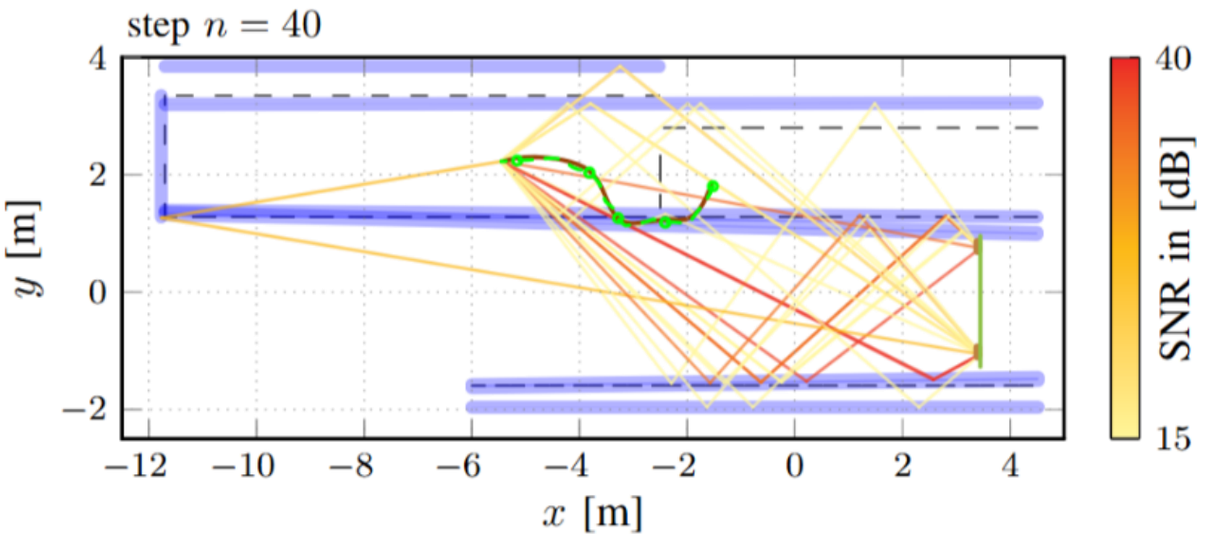

Agent RMSE

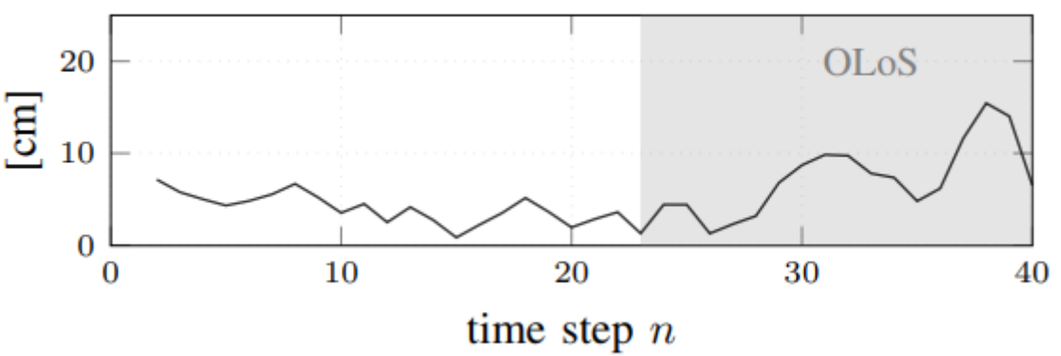

Synthetic Data

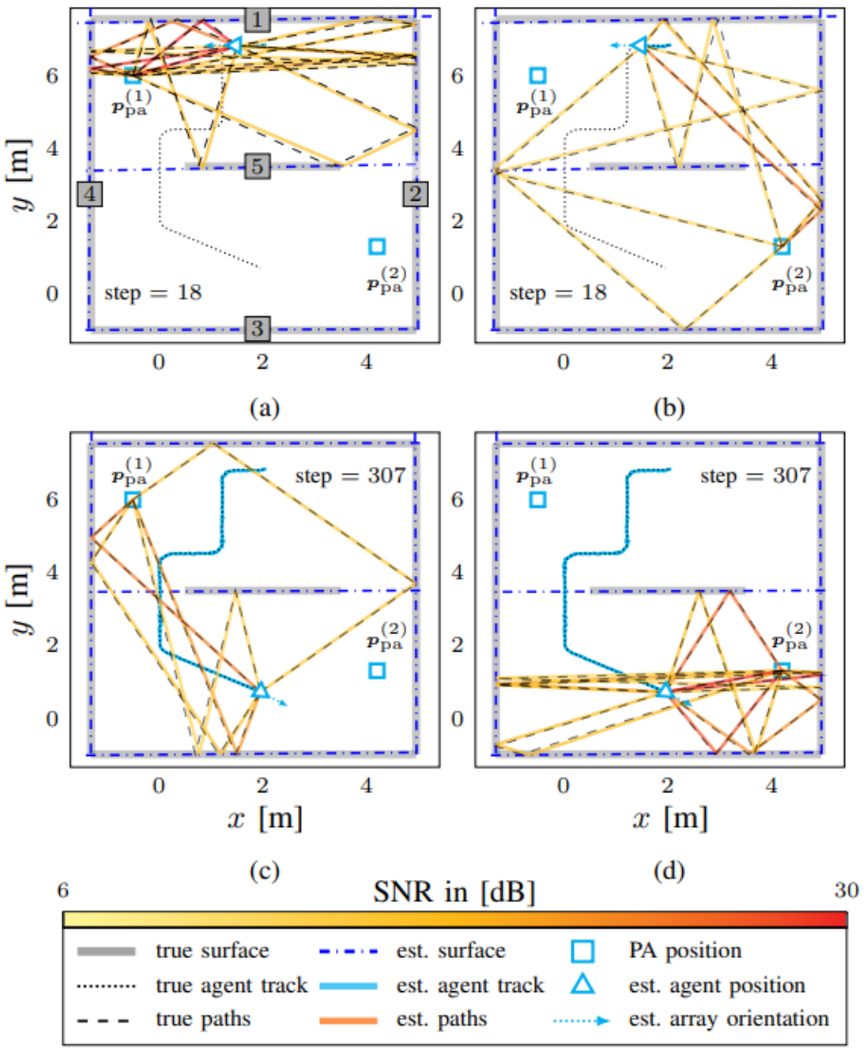

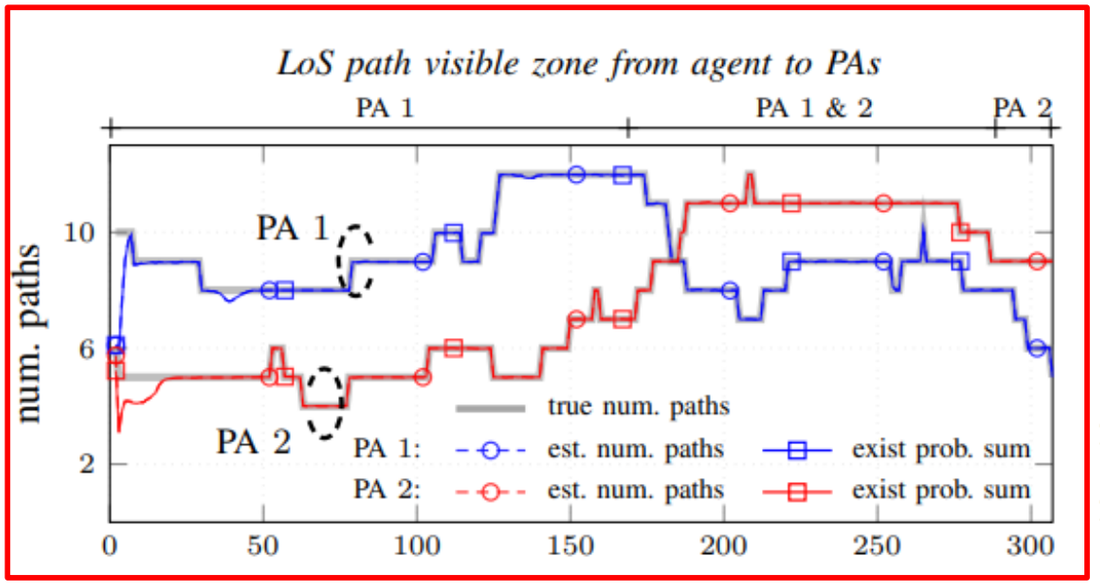

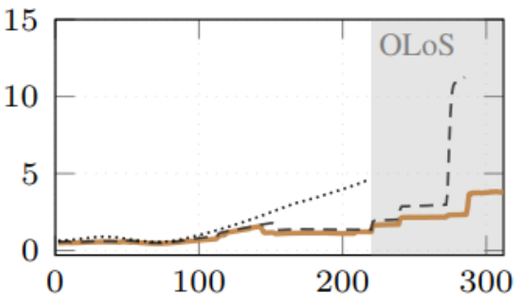

(d)

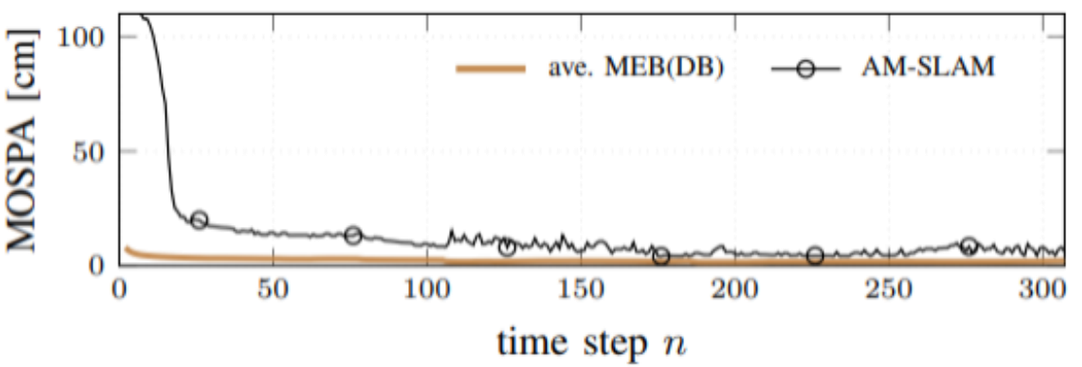

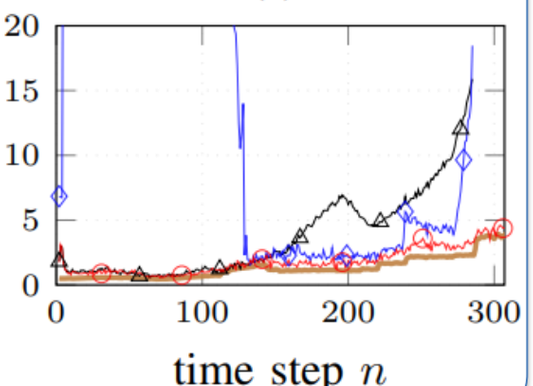

Coherent Direct MP-SLAM

Direct inference $\Rightarrow$ **signal model + probabilistic model**

Received radio signal at PA j:

$$\boldsymbol{z}_n^{(j)} = \sum_{s \in S_n} r_{s,n} r_{s,n}^{(j)} \rho_{s,n} \boldsymbol{\psi}^{(j)}(\boldsymbol{p}_n, \boldsymbol{p}_s^{\mathrm{sfv}}) + \boldsymbol{w}_n^{(j)} \qquad \in \mathbb{C}^{N_{\mathrm{z}}}$$

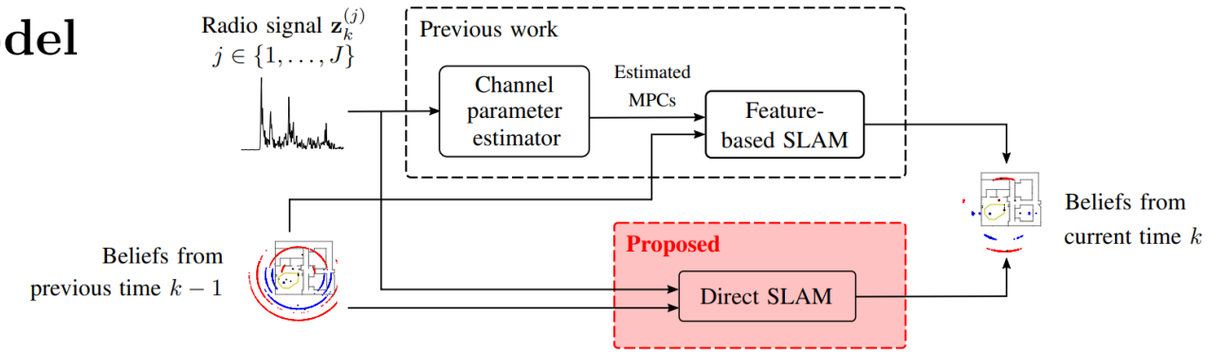

- Implicitly absorbs all effects in the signal model

  $\rightarrow$ SFV-related existence $r_{s,n}$ and path-related existence $r_{s,n}^{(j)}$

  $\rightarrow$ Noise-related parameters such as variance $\eta_n^{(j)}$

  $\rightarrow$ Complex amplitude model: $\rho_{s,n}^{(j)} \sim \mathcal{CN}(\mu_{s,n}, \gamma_{s,n})$

  - Variance $\gamma_{s,n}$ $\rightarrow$ accounts for "non-coherent power"
  - Mean value $\mu_{s,n}$ $\rightarrow$ enables coherent processing for large-aperture/D-MIMO systems

B. J. B. Deutschmann, E. Leitinger, and K. Witrisal, "Soft Coherent Multipath-based SLAM," arXiv, 2026.

M. Liang, E. Leitinger and F. Meyer, "Direct Multipath-Based SLAM," in IEEE Transactions on Signal Processing, vol. 73, pp. 2336-2352, 2025, doi: 10.1109/TSP.2025.3552747

Coherent Direct MP-SLAM

- Type-II likelihood function with mean:

$$f(\mathbf{z}_n^{(j)}|\mathbf{x}_n, \mathbf{y}_n, \mathbf{r}_n^{(j)}, \eta_n^{(j)}) = \mathcal{CN}\left(\mathbf{z}_n^{(j)}; \boldsymbol{\mu}_n^{(j)}, \mathbf{C}_n^{(j)}\right)$$

- Mean value: $\boldsymbol{\mu}_n^{(j)} = \sum_{s\in\tilde{\mathcal{S}}_n} r_{s,n}\, r_{s,n}^{(j)}\, \mu_{s,n}\, \boldsymbol{\psi}^{(j)}\left(\mathbf{x}_n, \mathbf{p}_{s,\text{sfv}}\right)$

- Covariance matrix: $\mathbf{C}_n^{(j)} = \eta_n^{(j)}\mathbf{I}_{N_z} + \sum_s r_{s,n}\, r_{s,n}^{(j)}\, \gamma_{s,n}\, \boldsymbol{\psi}^{(j)}\left(\mathbf{x}_n, \mathbf{p}_{s,\text{sfv}}\right)\boldsymbol{\psi}^{(j)}\left(\mathbf{x}_n, \mathbf{p}_{s,\text{sfv}}\right)^{\text{H}}$

- **Local** spherical coordinates PA j: $\acute{\boldsymbol{r}}_{s,n}^{(j)} = \boldsymbol{M}_j^{-1}\tilde{\boldsymbol{r}}_{s,n}^{(j)}(\boldsymbol{p}_n, \boldsymbol{p}_{s,\text{sfv}})$

$$\tau_{s,n}^{(j)} = \frac{\|\acute{\boldsymbol{r}}_{s,n}^{(j)}\|}{\text{c}}$$

$$\theta_{s,n}^{(j)} = \arccos\left([\acute{\boldsymbol{r}}_{s,n}^{(j)}]_3 / \|\acute{\boldsymbol{r}}_{s,n}^{(j)}\|\right)$$

$$\vartheta_{s,n}^{(j)} = \text{atan2}\left([\acute{\boldsymbol{r}}_{s,n}^{(j)}]_2, [\acute{\boldsymbol{r}}_{s,n}^{(j)}]_1\right)$$

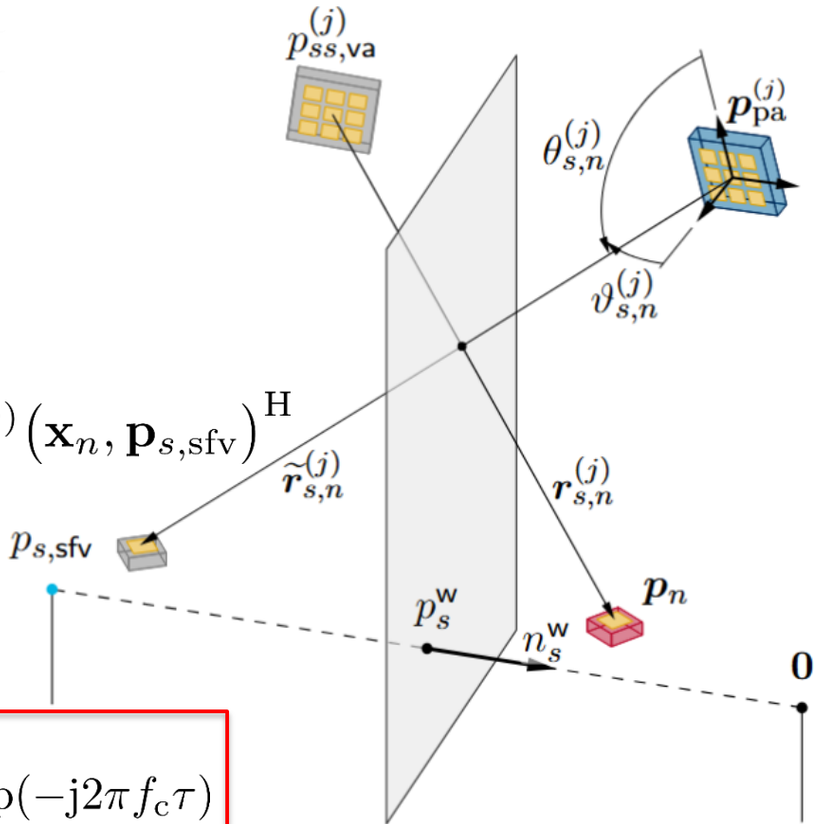

Local planar-array:
$\boldsymbol{\psi}(\boldsymbol{\theta}) = \frac{\lambda}{4\pi\tau} S(\mathbf{f}) \odot \left(\exp(\text{j}2\pi\mathbf{f}\tau) \otimes \boldsymbol{a}(\theta, \vartheta)\right) \exp(-\text{j}2\pi f_c \tau)$

↓

Global spherical-array: Data fusion with mean values of LHF (LOS and SFVs)

⇒ Parameters $\boldsymbol{\theta}_{s,n}^{(j)}$ within the signal $\boldsymbol{z}_n^{(j)}$ are a function of agent position $\boldsymbol{p}_n$ and SFVs positions $\boldsymbol{p}_{s,\text{sfv}}$

Joint Posterior PDF and Factor Graph

- Joint inference of agent state $\mathbf{x}_{0:n}$, PSFV states $\mathbf{y}_{0:n}$, PR states $\boldsymbol{r}_{0:n}$, noise variance $\boldsymbol{\eta}_{1:n}$
  - Joint posterior PDF: $f\left(\mathbf{x}_{0:n}, \mathbf{y}_{0:n}, \boldsymbol{r}_{0:n}, \boldsymbol{\eta}_{0:n} | \mathbf{z}_{1:n}\right)$
  - Marginal posterior PDFs:
    $p(r_{s,n} = 1|\mathbf{z}_{1:n})$, $p(r^{(j)}_{ss',n} = 1|\mathbf{z}_{1:n})$, $f(\mathbf{p}_{s,\text{sfv}}|r_{s,n} = 1, \mathbf{z}_{1:n})$, $f(\mathbf{x}_n|\mathbf{z}_{1:n})$, $f(\eta^{(j)}_n|\mathbf{z}_{1:n})$
- Factorization of joint posterior PDF $\Rightarrow$ factor graph

  $\rightarrow$ Message passing algorithm + particle-based implementation to approximate marginal PDFs

  $\rightarrow$ Efficient implementation exploiting matrix inversion lemma and GPU

  $\rightarrow$ MMSE estimation

Factor Graph

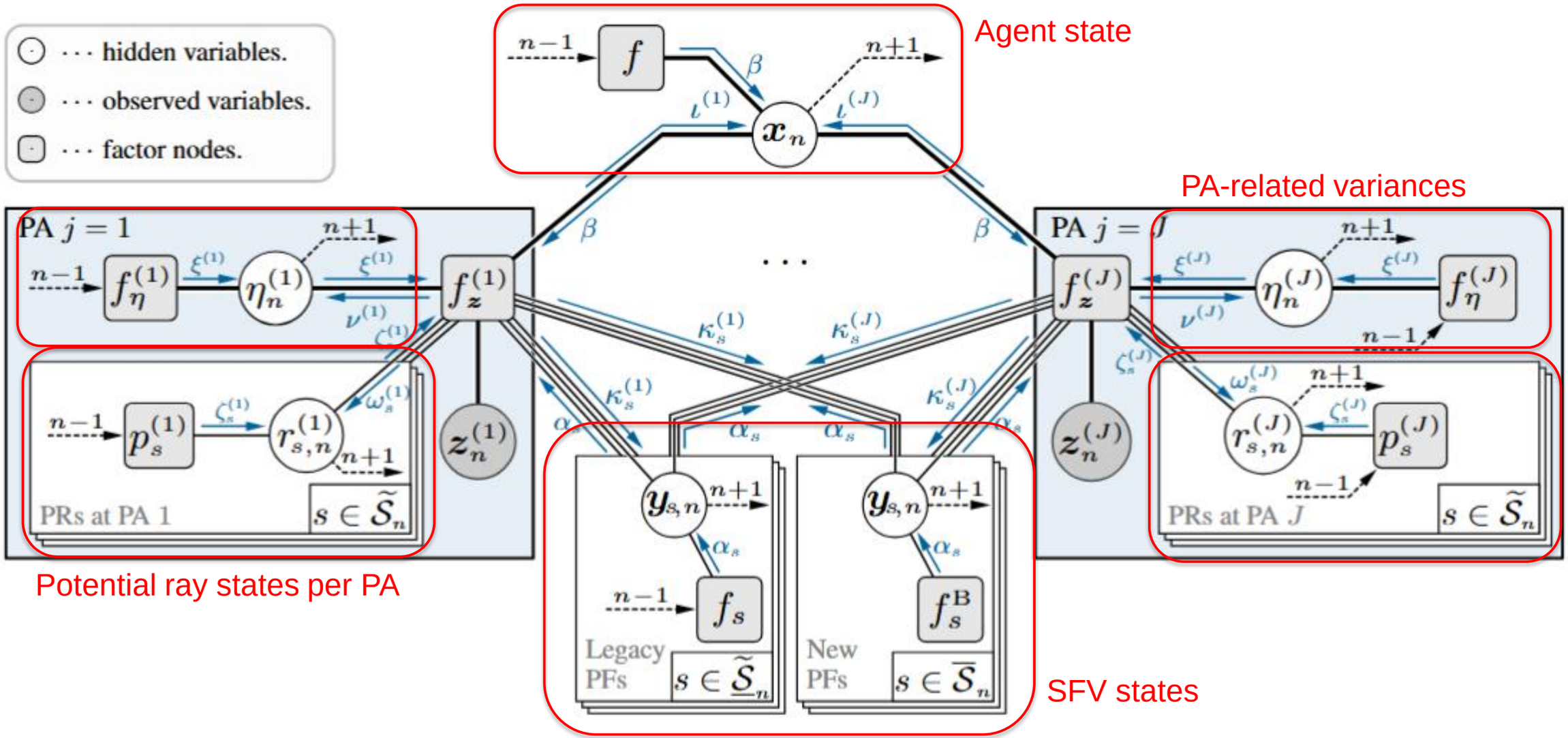

$\Rightarrow$ Additional synchronization parameters such as clock and timing offsets of PAs can be incorporated as well!

A. Fascista et al., "Joint localization, synchronization and mapping via phase-coherent distributed arrays," IEEE J. Sel. Topics Signal Process., pp. 1–16, Jan. 2025.

Numerical Simulations

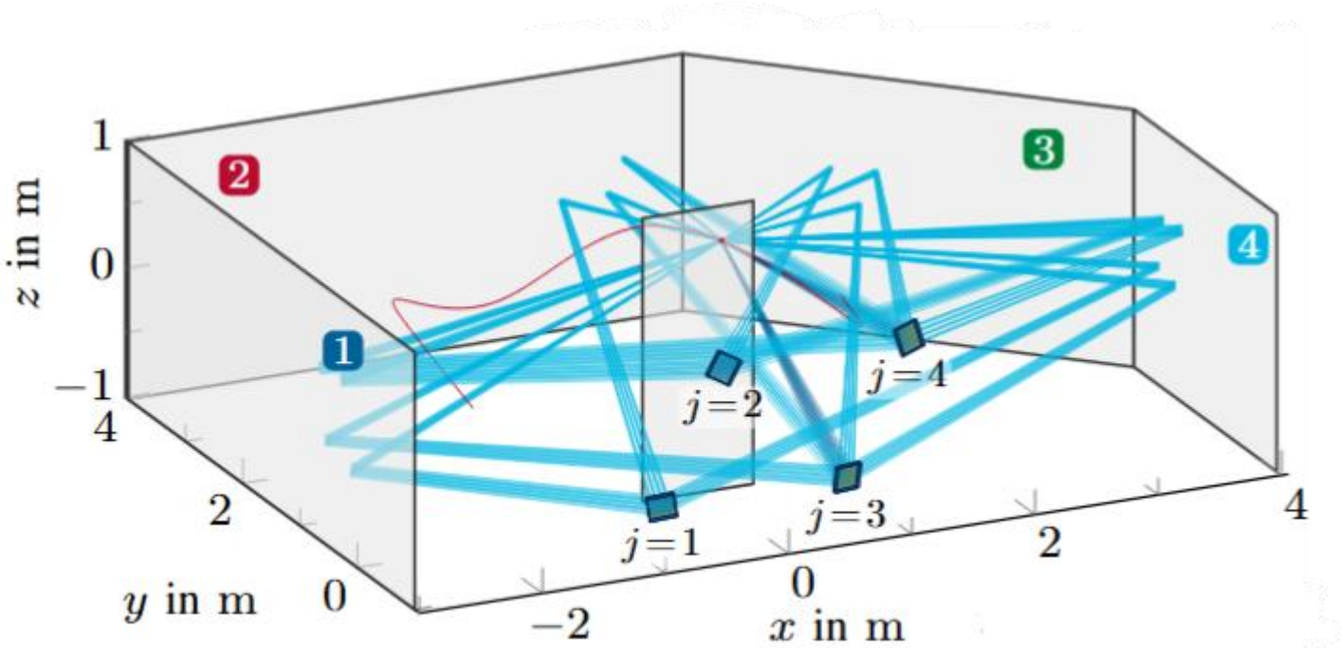

System Parameters:

- Number of PAs $J = 4$
- Bandwidth $B = 100\,\mathrm{MHz}$
- Carrier frequency $f_c = 3.5\,\mathrm{GHz}$
- URA $(M_y \times M_z) = (4 \times 4)$ at $\lambda/2$ spacing

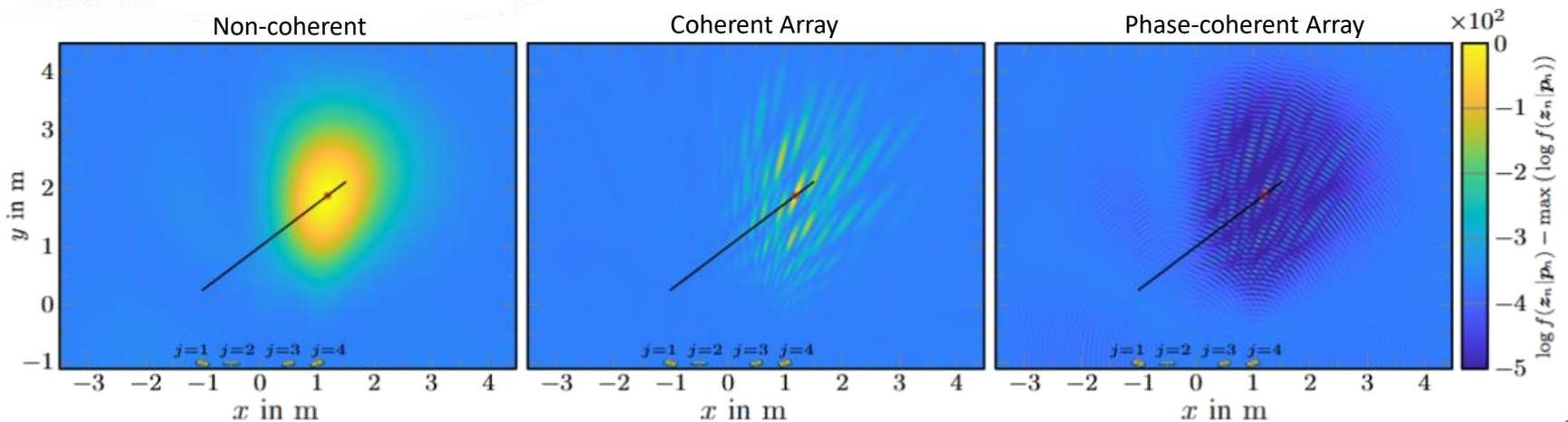

Numerical Simulations

Agent RMSE:

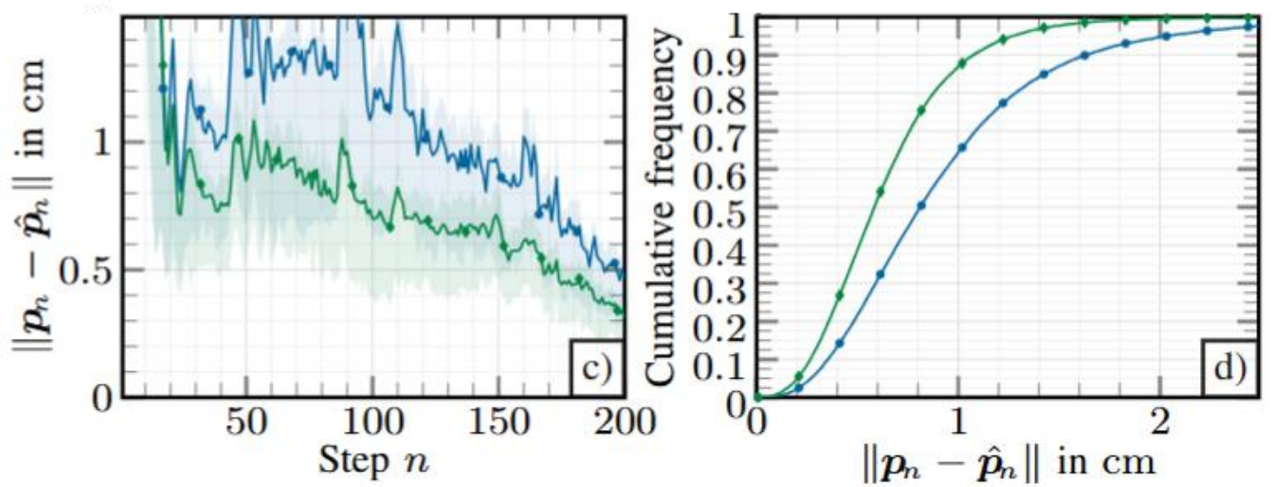

Path-existences:

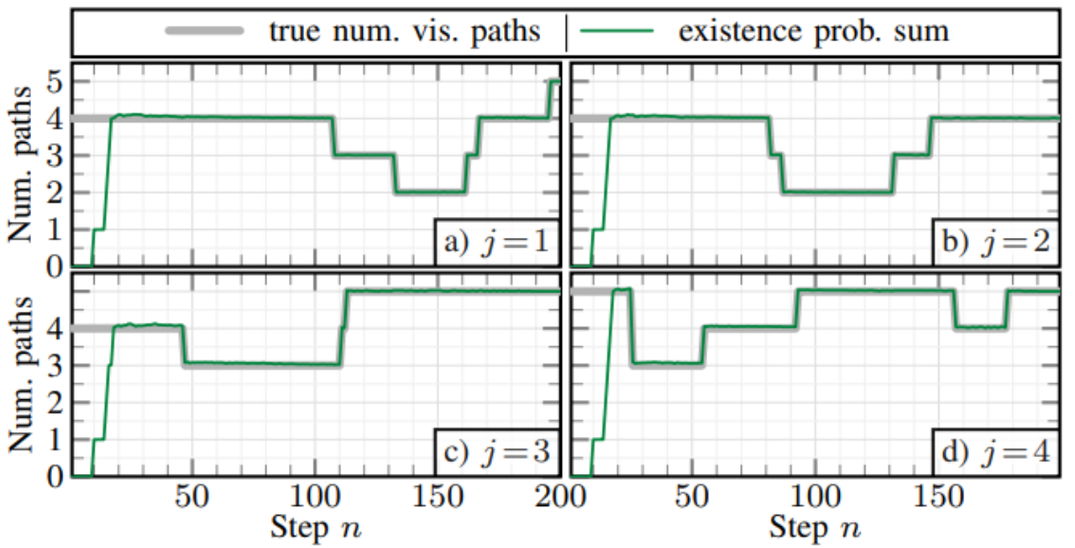

SFV RMSE:

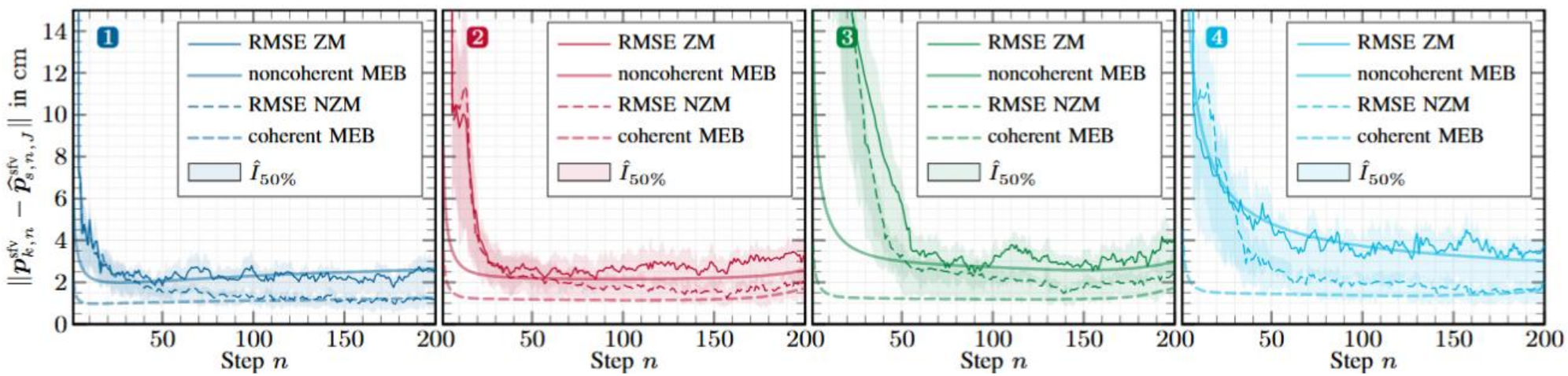

Hybrid Graph-based Inference with Learned Models

Data-driven and model-free

Machine learning

training factor graph-intrinsic cost-function

model-based likelihoods and priors combined with ML

Data (training)

Current meas.

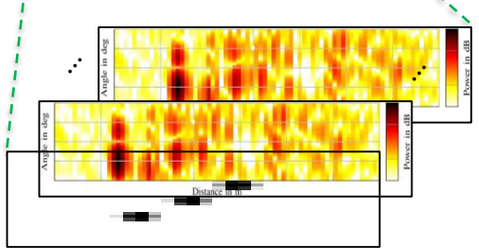

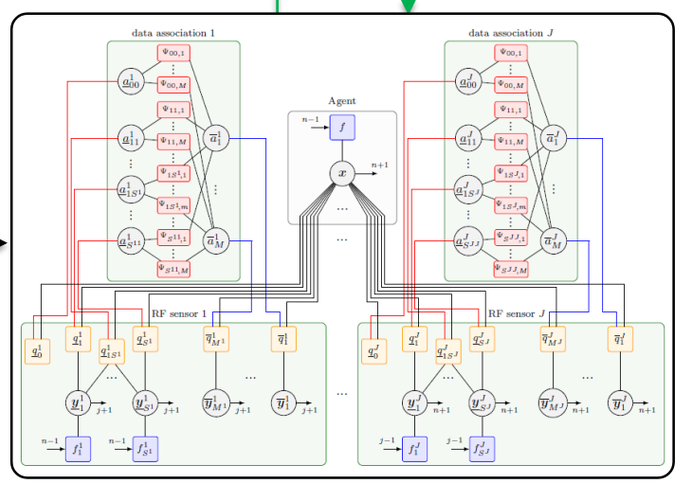

Model-based factor graph

Large-scale Environment

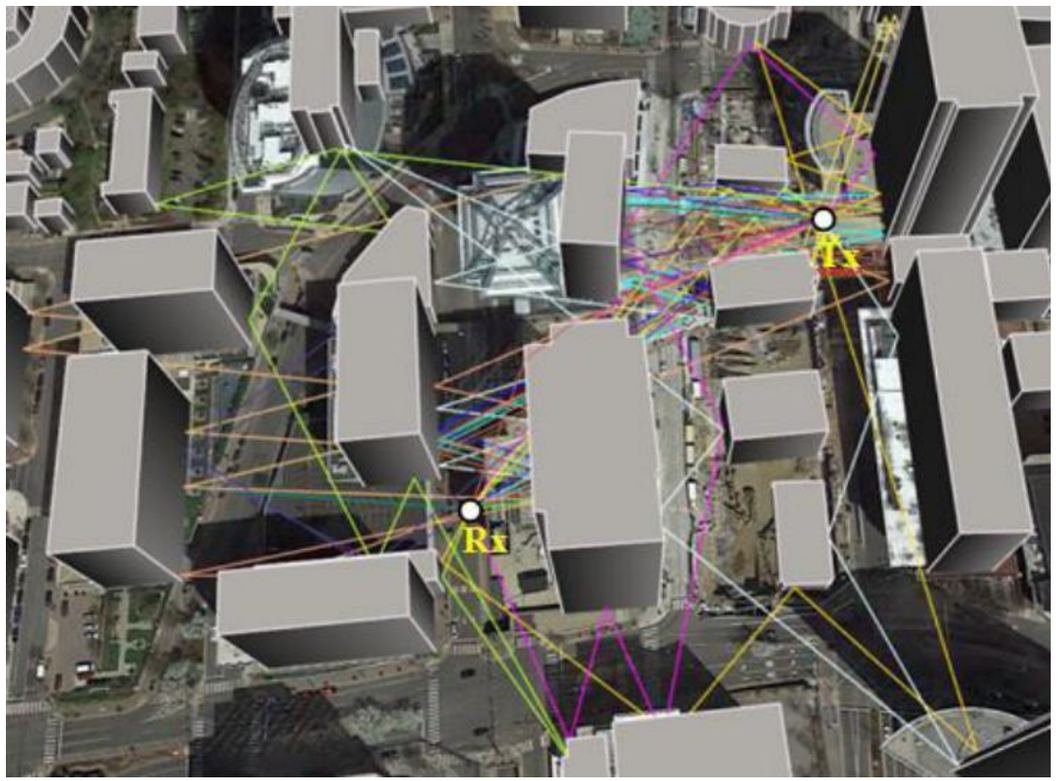

Account for model-mismatch, hardware impairments, …

MP-SLAM with Probabilistic Occupancy-grid

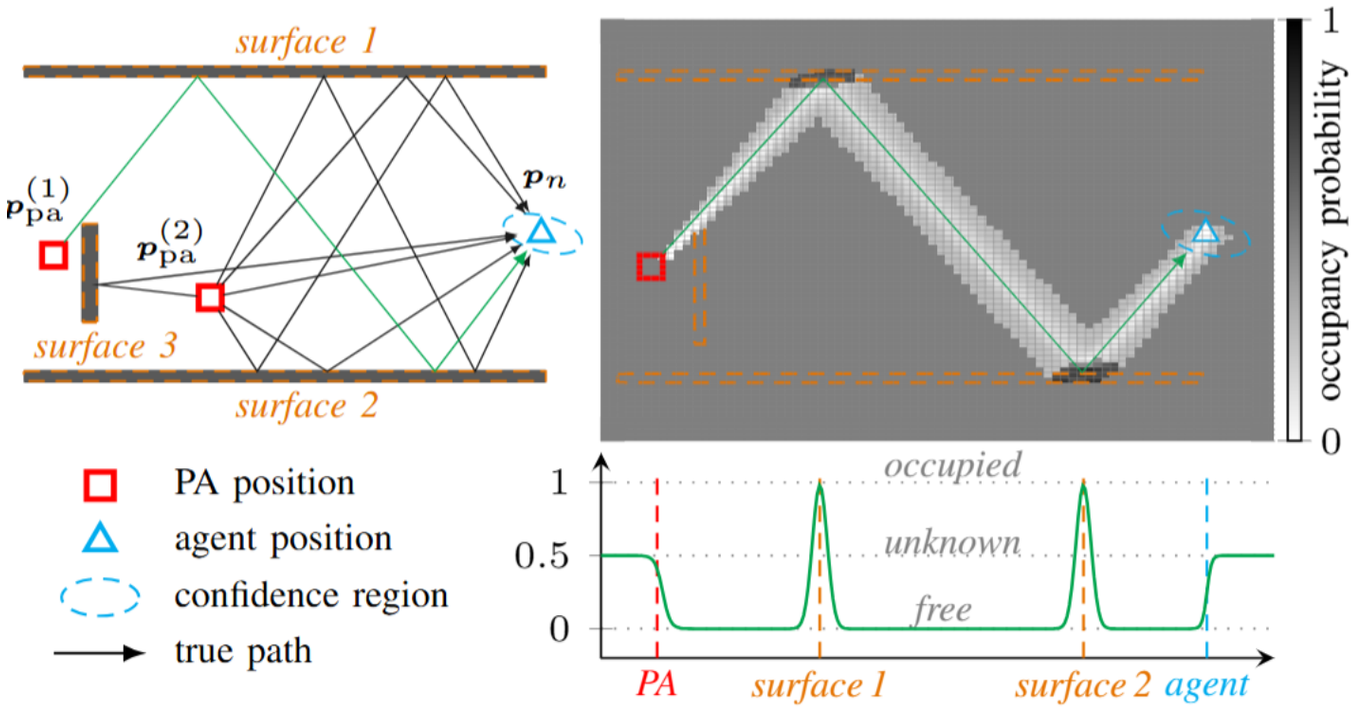

First step toward a general map represented by a learned model

- **SFV-based data fusion:** SFVs (again) enable consistent fusion of single-bounce paths, double-bounce paths, and PAs
- **SFV-based amplitudes:** SFVs have reflection coefficients → normalized path amplitudes
- **Occupancy ⇒ visibility:** Grid-cell occupancy implicitly captures path existence/visibility replacing explicit two-layer models

X. Li, E. Leitinger, F. Tufvesson, and F. Meyer, "Probabilistic occupancy grid for radio-based SLAM," arXiv, 2026.

Extension of Factor Graph

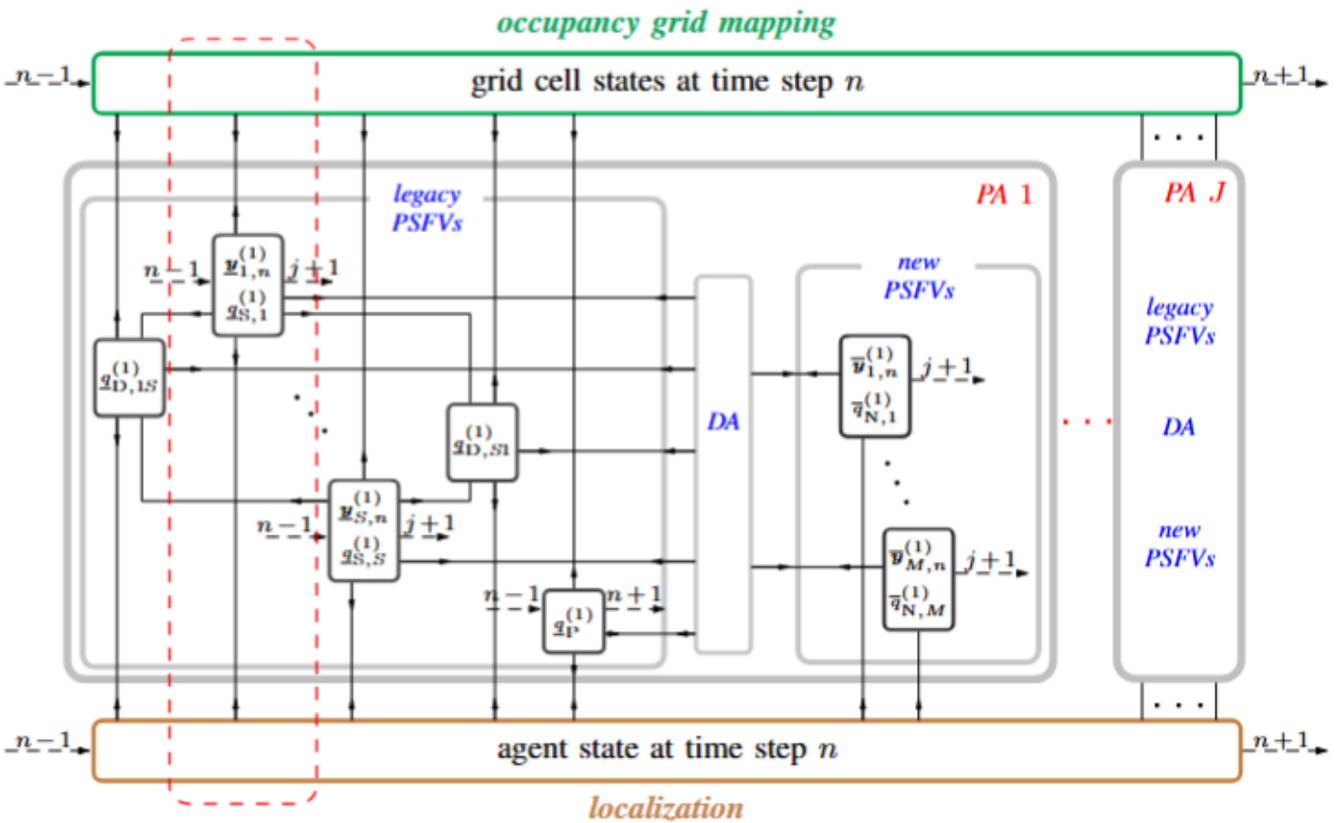

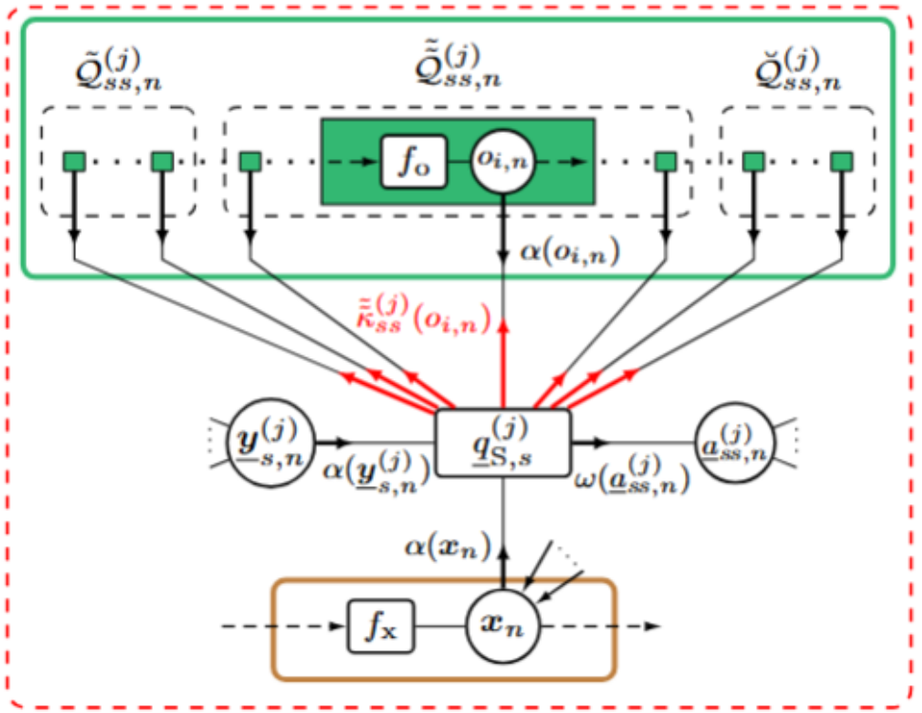

- **Bayesian inference:** Agent, SFVs, and occupancy states inference via factor graphs

Results

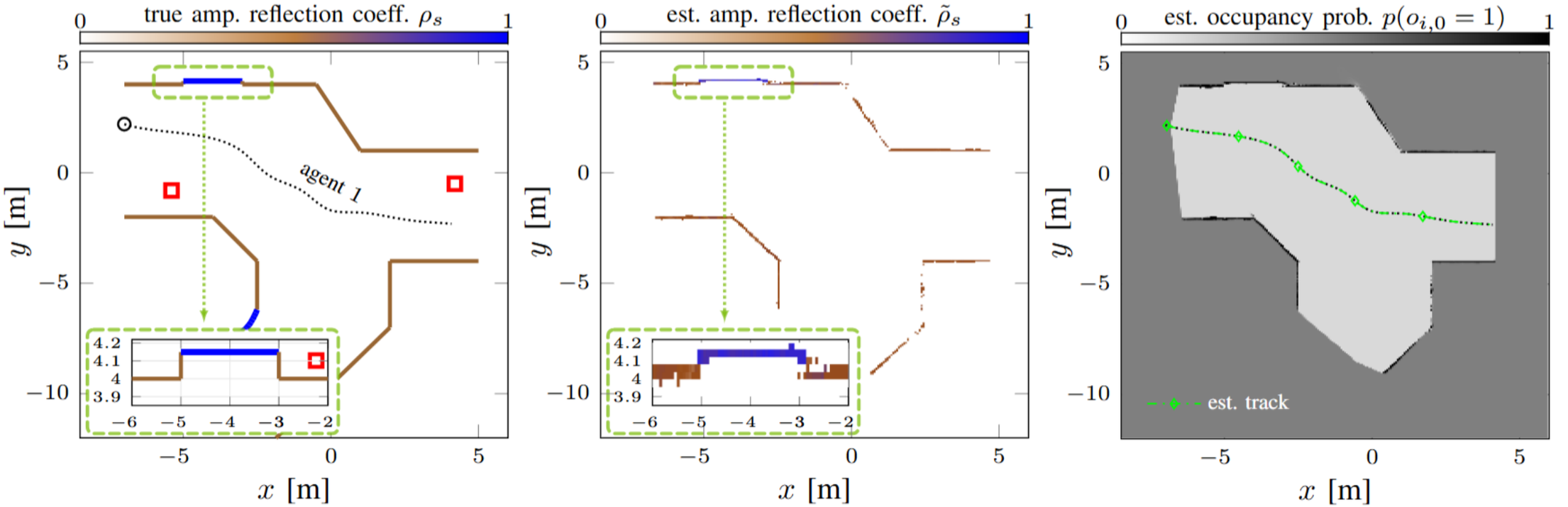
true amp. reflection coeff. ρ_s
0
1
agent 1
y [m]
x [m]
est. amp. reflection coeff. $\tilde{\rho}_s$
est. occupancy prob. $p(o_{i,0} = 1)$
est. track

Results

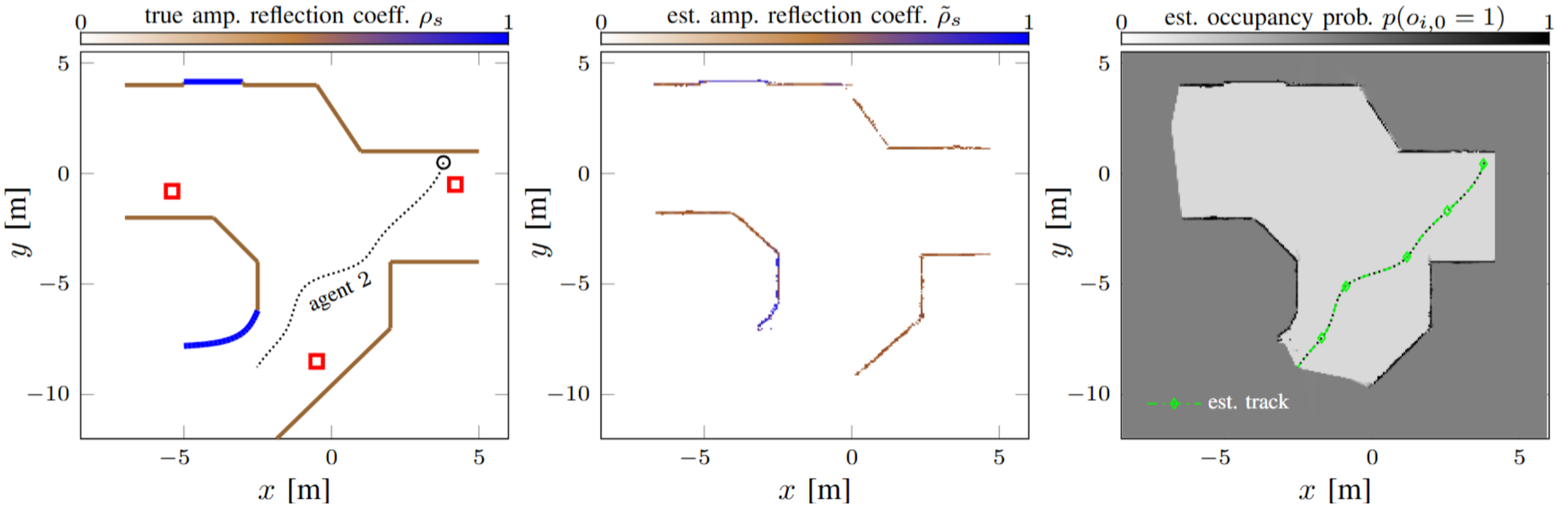
true amp. reflection coeff. ρ_s
0
1
agent 2
est. amp. reflection coeff. $\tilde{\rho}_s$
est. occupancy prob. $p(o_{i,0} = 1)$
est. track
x [m]
y [m]
5
0
−5
−10

Results

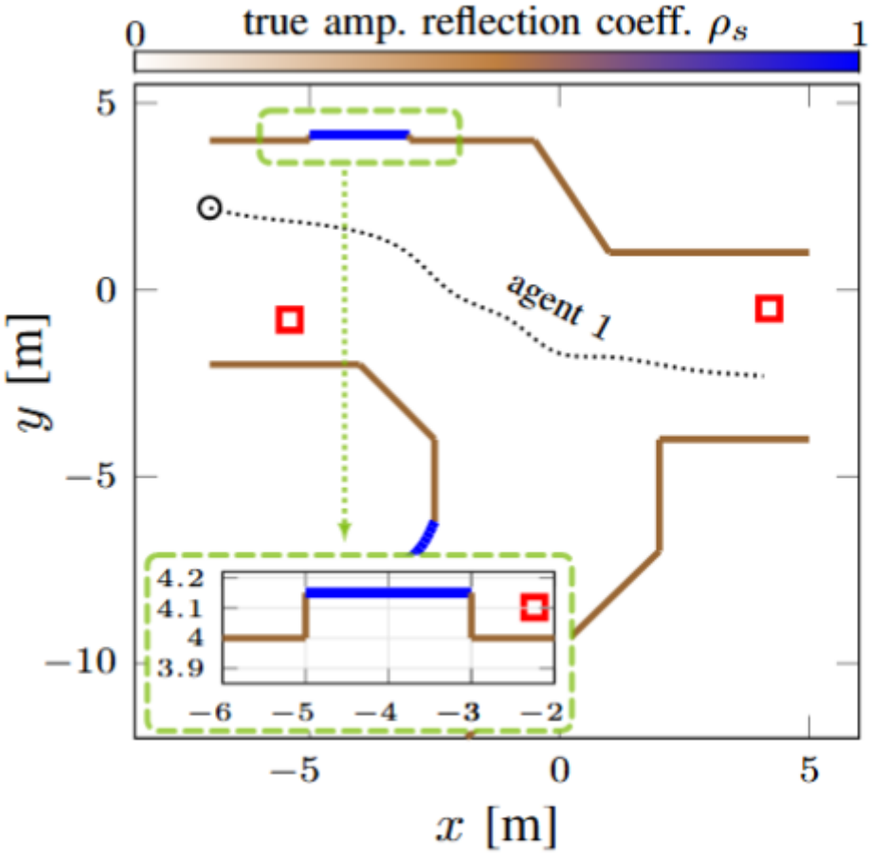
0
true amp. reflection coeff. ρ_s
1
5
0
−5
−10
y [m]
agent 1
4.2
4.1
4
3.9
−6
−5
−4
−3
−2
−5
0
5
x [m]

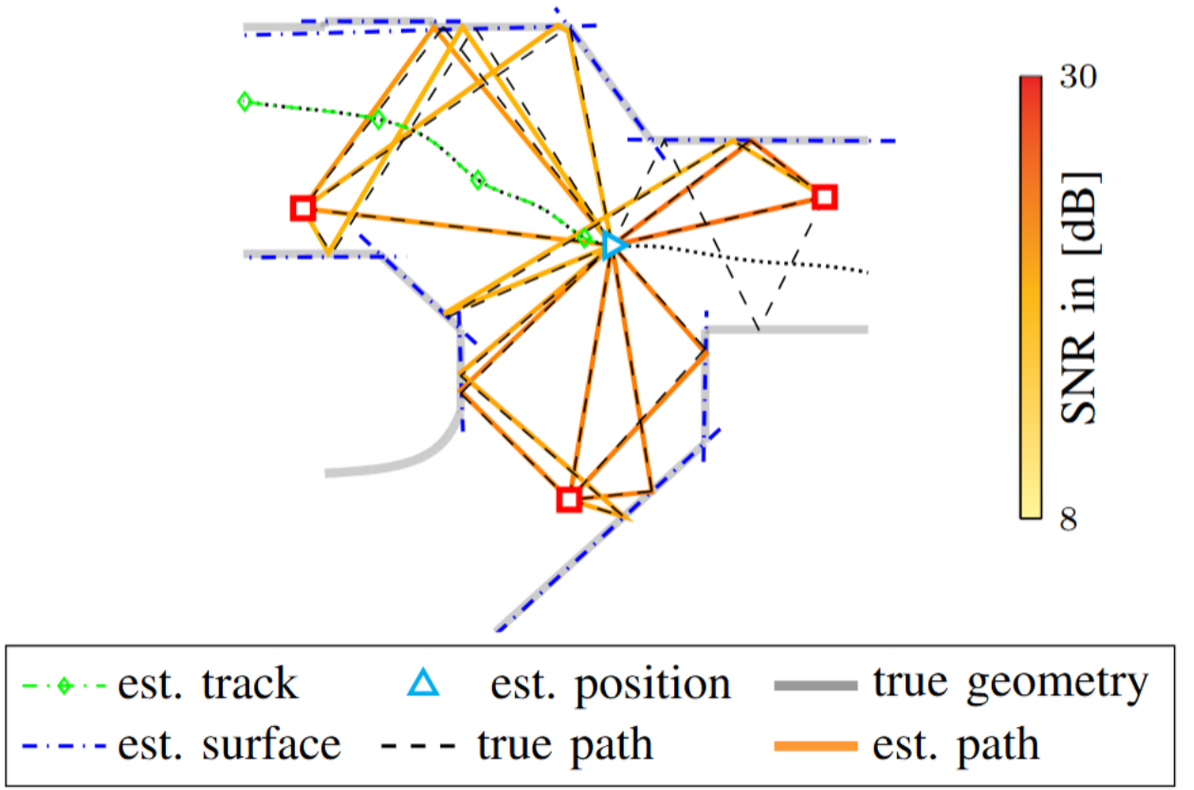
30
SNR in [dB]
8
est. track
est. position
true geometry
est. surface
true path
est. path

Unsupervised Learning for AI-enhanced Direct SLAM

- The model combines
  - **model-based part** → known LOS physics and the steering vector
  - **learned part** → captures environment-induced multipath and potentially unknown array calibration parameters (learned model)

- Graph-based inference algorithm estimates the agent state, while AI model is learned unsupervised from the measurement evidence

Key idea: Preserve the physical structure where it is known, and learn only the difficult environment-dependent part

A. Venus, B. Deutschmann, A. Fuchs, C. Knoll, and E. Leitinger,"AI-enhanced direct SLAM: A principled approach to unsupervisedlearning in Bayesian inference," arXiv, 2026.

Signal Model

Direct MP-SLAM approach based on signal:

$$\boldsymbol{z}_n^{(j)} = \sum_{l=1}^{L_n^{(j)}} \varrho_{l,n}^{(j)}\, \boldsymbol{h}_{\boldsymbol{\chi}}\left(\tau_{l,n}^{(j)}, \boldsymbol{u}_{l,n}^{(j)}\right) + \boldsymbol{\epsilon}_n^{(j)}$$

- $\boldsymbol{h}_{\boldsymbol{\chi}}(\tau, \boldsymbol{u}) = \boldsymbol{h}_{\boldsymbol{\chi}_\mathrm{f}}(\tau) \otimes \boldsymbol{a}_{\boldsymbol{\chi}_\mathrm{u}}(\boldsymbol{u})$ with $M = M_\mathrm{f} M_\mathrm{a}$
- $\boldsymbol{\epsilon}_n^{(j)} \sim \mathcal{CN}(\mathbf{0}, \eta_n^{(j)} \boldsymbol{I})$
- $\boldsymbol{\chi}$ unknown array calibration parameter

$$\mathbf{h}_{\boldsymbol{\chi}_\tau}(\tau) = \frac{1}{4\pi f_c \tau}\big[w_{f,1}\, S(-(M_f-1)\Delta/2)\, e^{j2\pi(-(M_f-1)\Delta/2)\tau} \cdots\ w_{f,M_f}\, S((M_f-1)\Delta/2)\, e^{-j2\pi((M_f-1)\Delta/2)\tau}\big]^\mathrm{T}$$

$$\mathbf{a}_{\boldsymbol{\chi}_u}(\mathbf{u}) = \big[w_{u,1}\, e^{-j\frac{2\pi}{\lambda_c}\mathbf{u}^\top(\mathbf{a}_1+\Delta\mathbf{a}_1)} \cdots\ w_{u,M_u}\, e^{-j\frac{2\pi}{\lambda_c}\mathbf{u}^\top(\mathbf{a}_{M_u}+\Delta\mathbf{a}_{M_u})}\big]^\mathrm{T}$$

$$\boldsymbol{\chi} = [\boldsymbol{\chi}_f^\mathrm{T}\ \boldsymbol{\chi}_u^\mathrm{T}]^\mathrm{T}$$

$$\boldsymbol{\chi}_f = [w_{f,1}\ \cdots\ w_{f,M_f}]^\mathrm{T}$$

$$\boldsymbol{\chi}_u = [w_{u,1}\ \cdots\ w_{u,M_u}\ \Delta a_1^\mathrm{T}\ \cdots\ \Delta a_{M_u}^\mathrm{T}]^\mathrm{T}$$

Inference Signal Model

Separating line-of-sight (LOS) and environment-induced multipath components:

$$\underbrace{\boldsymbol{z}_n^{(j)}}_{\text{raw signal}} = \underbrace{r_n^{(j)} \rho_{\text{lo},n}^{(j)} \boldsymbol{h}_{\boldsymbol{\chi}}^{\text{lo}(j)}(\boldsymbol{p}_n)}_{\text{physics-based LOS}} + \underbrace{\sum_{i=1}^{D} \rho_{\boldsymbol{\theta},i}^{\text{ai}(j)} \boldsymbol{h}_{\tilde{\boldsymbol{\theta}},i}^{\text{ai}(j)}(\boldsymbol{p}_k)}_{\text{learned environment model}} + \boldsymbol{\epsilon}_n^{(j)}$$

- $r_n^{(j)}$ existence variable models LOS visibility and $\rho_{\text{lo},k}^{(j)} \sim \mathcal{CN}\left(\rho_{\text{lo},k}^{(j)}; 0, \gamma_k^{(j)}\right)$
- $\boldsymbol{h}_{\boldsymbol{\chi}}^{\text{lo}(j)}(\boldsymbol{p}_n) \triangleq \boldsymbol{h}_{\boldsymbol{\chi}}\left(\tau_{\text{lo},n}^{(j)}, \boldsymbol{u}_{\text{lo},n}^{(j)}\right)$ determined by the LOS delay and direction
  - LOS delay: $\tau_{\text{lo},n}^{(j)} = \|\boldsymbol{p}^{(j)} - \boldsymbol{p}_n\|/c$
  - LOS DoA: $\boldsymbol{u}_{\text{lo},n}^{(j)} = \boldsymbol{R}(o_n)(\boldsymbol{p}^{(j)} - \boldsymbol{p}_n)/\|\boldsymbol{p}^{(j)} - \boldsymbol{p}_n\|$

Inference Signal Model

Separating line-of-sight (LOS) and environment-induced multipath components:

$$\underbrace{\boldsymbol{z}_n^{(j)}}_{\text{raw signal}} = \underbrace{r_n^{(j)} \rho_{\text{lo},n}^{(j)} \boldsymbol{h}_{\boldsymbol{\chi}}^{\text{lo}(j)}(\boldsymbol{p}_n)}_{\text{physics-based LOS}} + \underbrace{\sum_{i=1}^{D} \rho_{\boldsymbol{\theta},i}^{\text{ai}(j)} \boldsymbol{h}_{\tilde{\boldsymbol{\theta}},i}^{\text{ai}(j)}(\boldsymbol{p}_k)}_{\text{learned environment model}} + \boldsymbol{\epsilon}_n^{(j)} \qquad \text{with } \tilde{\boldsymbol{\theta}} = [\boldsymbol{\chi}^{\text{T}} \boldsymbol{\theta}^{\text{T}}]^{\text{T}}$$

- Complex amplitudes $\rho_{\boldsymbol{\theta},n,k}^{\text{ai}(j)} \sim \mathcal{CN}\big(\rho_{\boldsymbol{\theta},n}^{\text{ai}(j)}; 0, \gamma_{\boldsymbol{\theta},n}^{\text{ai}(j)}\big)$

  $\rightarrow \boldsymbol{\gamma}_{\boldsymbol{\theta}}^{\text{ai}(j)} = f_{\rho,\boldsymbol{\theta}}^{\text{ai}}(\boldsymbol{p}^{(j)}) \in \mathbb{R}_+^D$

  DNN predicts power-related variances

- $\boldsymbol{h}_{\tilde{\boldsymbol{\theta}},i}^{\text{ai}(j)}(\boldsymbol{p}_n) \triangleq \boldsymbol{h}_{\boldsymbol{\chi}}\big(\tau_{\boldsymbol{\theta},i,n}^{\text{ai}(j)}, \boldsymbol{u}_{\boldsymbol{\theta},i,n}^{\text{ai}(j)}\big)$ models environment-induced MPCs generated by the learned map

  $\rightarrow \boldsymbol{P}_{\boldsymbol{\theta}}^{\text{ai}(j)} = f_{\boldsymbol{p},\boldsymbol{\theta}}^{\text{ai}}(\boldsymbol{p}^{(j)}) \in \mathbb{R}^{(d+1)\times D}$

  DNN predicts feature locations and delay biases

  - $\boldsymbol{\tau}_{\boldsymbol{\theta},i,n}^{\text{ai}(j)} = \|\boldsymbol{p}_{\boldsymbol{\theta},i}^{\text{ai}(j)} - \boldsymbol{p}_n\|/c + b_{\boldsymbol{\theta},i}^{\text{ai}(j)}$
  - $\boldsymbol{u}_{\boldsymbol{\theta},i,n}^{\text{ai}(j)} = \boldsymbol{R}(o_k)(\boldsymbol{p}_{\boldsymbol{\theta},i}^{\text{ai}(j)} - \boldsymbol{p}_n)/\|\boldsymbol{p}_{\boldsymbol{\theta},i}^{\text{ai}(j)} - \boldsymbol{p}_n\|$
  - $\boldsymbol{P}_{\boldsymbol{\theta}}^{\text{ai}(j)} = \big[[\boldsymbol{p}_{\boldsymbol{\theta},1}^{\text{ai}(j)\,\text{T}} b_{\boldsymbol{\theta},1}^{\text{ai}(j)}]^{\text{T}} \cdots [\boldsymbol{p}_{\boldsymbol{\theta},D}^{\text{ai}(j)\,\text{T}} b_{\boldsymbol{\theta},D}^{\text{ai}(j)}]^{\text{T}}\big]$

Statistical and AI Model

- Zero-mean type-II likelihood function

$$f_{\tilde{\boldsymbol{\theta}}}(\boldsymbol{z}_n^{(j)}|\boldsymbol{x}_n, \boldsymbol{y}_n^{(j)}, \eta_n^{(j)}) = \mathcal{CN}\left(\boldsymbol{z}_n^{(j)}; \mathbf{0}, \boldsymbol{C}_{\tilde{\boldsymbol{\theta}},n}^{(j)}\right)$$

- Covariance matrix: $\boldsymbol{C}_{\tilde{\boldsymbol{\theta}},n}^{(j)} = \eta_n^{(j)} \boldsymbol{I}_M + r_n^{(j)} \boldsymbol{C}_{\boldsymbol{\chi},n}^{(j)} + \boldsymbol{C}_{\tilde{\boldsymbol{\theta}},n}^{\mathrm{ai}(j)}$

  - LOS-related covariance matrix: $\mathbf{C}_{\boldsymbol{\chi},n}^{(j)}(\mathbf{p}_n, \gamma_n^{(j)}) = \gamma_n^{(j)} \mathbf{h}_{\boldsymbol{\chi},n}^{(j)}(\mathbf{p}_n) \left(\mathbf{h}_{\boldsymbol{\chi},n}^{(j)}(\mathbf{p}_n)\right)^H$

  - AI-enhanced map-related covariance matrix: $\mathbf{C}_{\boldsymbol{\theta},n}^{\mathrm{ai}(j)}(\mathbf{p}_n) = \sum_{i=1}^{D} \gamma_{\boldsymbol{\theta},i}^{a(j)} \mathbf{h}_{\tilde{\boldsymbol{\theta}},n}^{\mathrm{ai}(j)}(\mathbf{p}_n) \left(\mathbf{h}_{\tilde{\boldsymbol{\theta}},i}^{\mathrm{ai}(j)}(\mathbf{p}_n)\right)^H$

Joint Posterior PDF and Factor Graph

- Joint inference of agent state $\boldsymbol{x}_{0:n}$, LOS states $\boldsymbol{y}_{0:n}$, noise variance $\boldsymbol{\eta}_{1:n}$
  - Joint posterior PDF: $f_{\tilde{\boldsymbol{\theta}}}(\boldsymbol{x}_{0:k}, \boldsymbol{y}_{0:k}, \boldsymbol{\eta}_{0:k} | \boldsymbol{z}_{1:k})$
  - Marginal posterior PDFs:
    $f(\boldsymbol{y}_n^{(j)} | \boldsymbol{z}_{1:n})$, $f(\boldsymbol{x}_n | \boldsymbol{z}_{1:n})$, $f(\eta_n^{(j)} | \boldsymbol{z}_{1:n})$
- Factorization of joint posterior PDF $\Rightarrow$ factor graph

  $\rightarrow$ Message passing algorithm + particle-based implementation to approximate marginal PDFs

  $\rightarrow$ Efficient implementation exploiting matrix inversion lemma

  $\rightarrow$ MMSE estimation

Unsupervised learning of AI Parameters

- The AI parameters $\tilde{\boldsymbol{\theta}} = [\boldsymbol{\chi}^{\mathrm{T}} \, \boldsymbol{\theta}^{\mathrm{T}}]^{\mathrm{T}}$ are learned by maximizing the evidence

$$\begin{aligned}\tilde{\boldsymbol{\theta}}^{\star} &= \arg\max_{\tilde{\boldsymbol{\theta}}} \log f_{\tilde{\boldsymbol{\theta}}}(\mathbf{z}_{1:n}) \\ &= \arg\max_{\tilde{\boldsymbol{\theta}}} \log \sum_{\mathbf{r}_{0:n}} \int \cdots \int f_{\tilde{\boldsymbol{\theta}}}(\mathbf{x}_{0:n}, \mathbf{r}_{0:n}, \mathbf{y}_{0:n}, \boldsymbol{\eta}_{0:n}, \mathbf{z}_{1:n}) \; d\mathbf{x}_{0:n} \, d\mathbf{y}_{0:n} \, d\boldsymbol{\eta}_{0:n}.\end{aligned}$$

- The evidence is approximated via the evidence lower bound (ELBO) and exploiting posterior PDF factorization:

$$\begin{aligned}Q(\tilde{\boldsymbol{\theta}}|\tilde{\boldsymbol{\theta}}_t) &\triangleq \mathbb{E}_{f_{\tilde{\boldsymbol{\theta}}_t}(\mathbf{x}_{0:n}, \mathbf{y}_{0:n}, \boldsymbol{\eta}_{0:n}|\mathbf{z}_{1:n})}[\log f_{\tilde{\boldsymbol{\theta}}}(\mathbf{x}_{0:n}, \mathbf{y}_{0:n}, \boldsymbol{\eta}_{0:n}, \mathbf{z}_{1:n})] \\ &= \sum_{k=1}^{n} \sum_{j=1}^{J} \mathbb{E}_{f_{\tilde{\boldsymbol{\theta}}_t}(\mathbf{x}_k, \mathbf{y}_k^{(j)}, \eta_k^{(j)}|\mathbf{z}_k)} \left[\log f_{\tilde{\boldsymbol{\theta}}}(\mathbf{z}_k^{(j)}|\mathbf{x}_k, \mathbf{y}_k^{(j)}, \eta_k^{(j)}) \right]\end{aligned}$$

- $Q(\tilde{\boldsymbol{\theta}}|\tilde{\boldsymbol{\theta}}_t) = \sum_{k=1}^{n} Q_k(\tilde{\boldsymbol{\theta}}|\tilde{\boldsymbol{\theta}}_t)$ depends on AI parameters $\tilde{\boldsymbol{\theta}}$ given "previous" AI parameters $\tilde{\boldsymbol{\theta}}_t$

Unsupervised learning of AI parameters

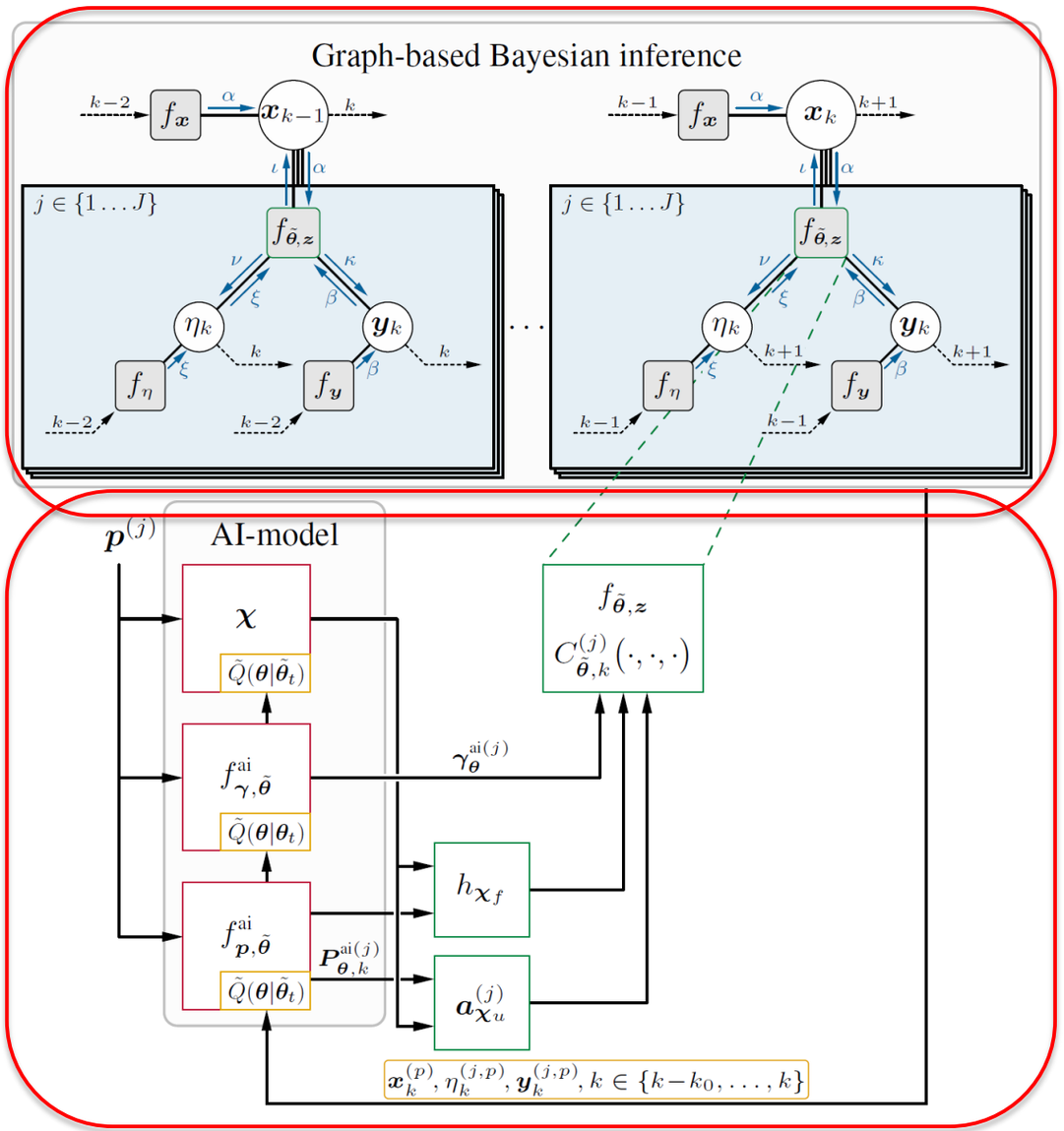

- **Inference step**: Posterior PDF $f_{\tilde{\boldsymbol{\theta}}_t}(\boldsymbol{x}_{0:n}, \boldsymbol{y}_{0:n}, \boldsymbol{\eta}_{0:n} | \boldsymbol{z}_{1:n})$ determined by FG-based message passing algorithm provides particle representations of marginal PDFs

- **Learning step**: $\tilde{\boldsymbol{\theta}}_{t+1}$ determined by maximizing

$$\tilde{\boldsymbol{\theta}}_{t+1} = \arg\max_{\tilde{\boldsymbol{\theta}}} \sum_{k=n-n_0}^{n_0} \tilde{Q}_k(\tilde{\boldsymbol{\theta}} | \tilde{\boldsymbol{\theta}}_t)$$

- $\tilde{Q}_k(\tilde{\boldsymbol{\theta}} | \tilde{\boldsymbol{\theta}}_t)$ particle-based approximation of $Q_k(\tilde{\boldsymbol{\theta}} | \tilde{\boldsymbol{\theta}}_t)$

Simulation Results

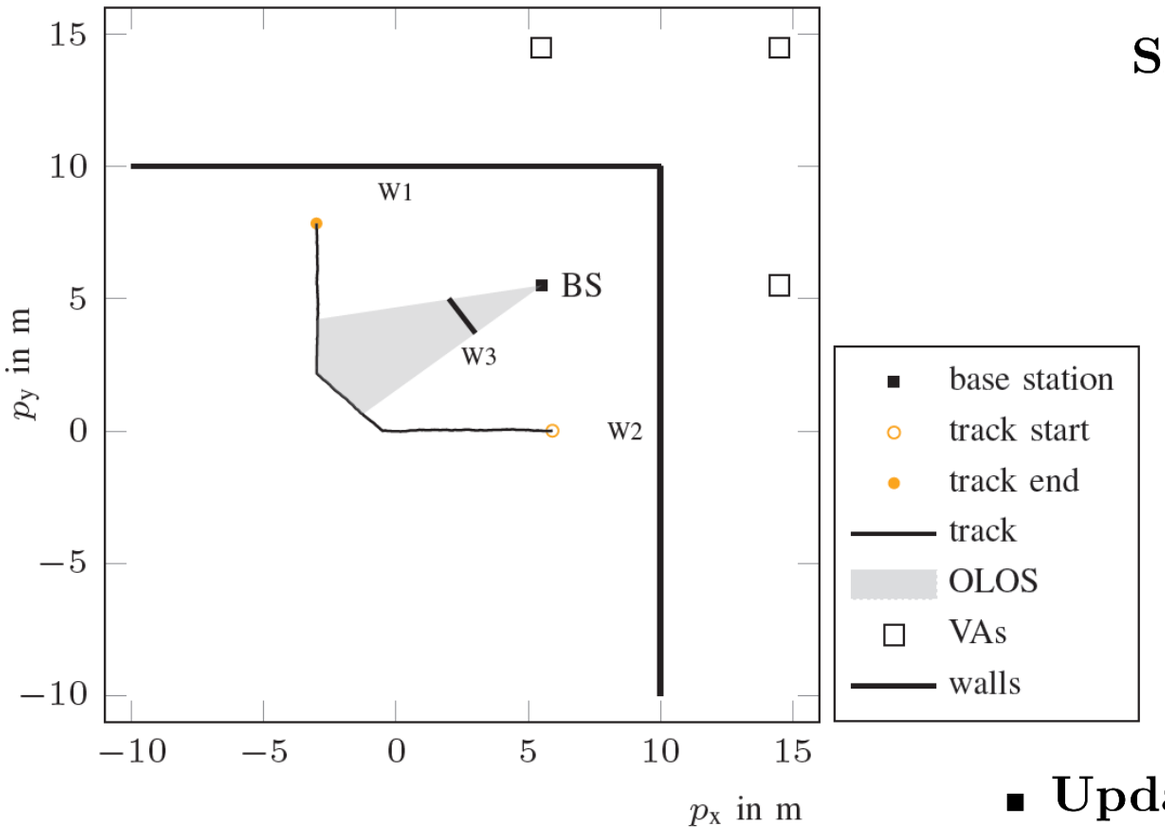

Simulation Parameters:

- Number of PAs $J = 1$
- Bandwidth 500 MHz, center frequency $f_c = 7$ GHz
- Uniform rectangular array with $\lambda/2$-spacing and $M_a = 4$ (agent)

- **Update interval:** $k_0 = 30$ time steps (track segment)
- **Particles:** $P = 5000$ inference, $P_0 = 30$ for learning
- **Training iterations:** 300 backpropagation steps per segment
- **AI model size:** $D = 30$ components

Simulation Results

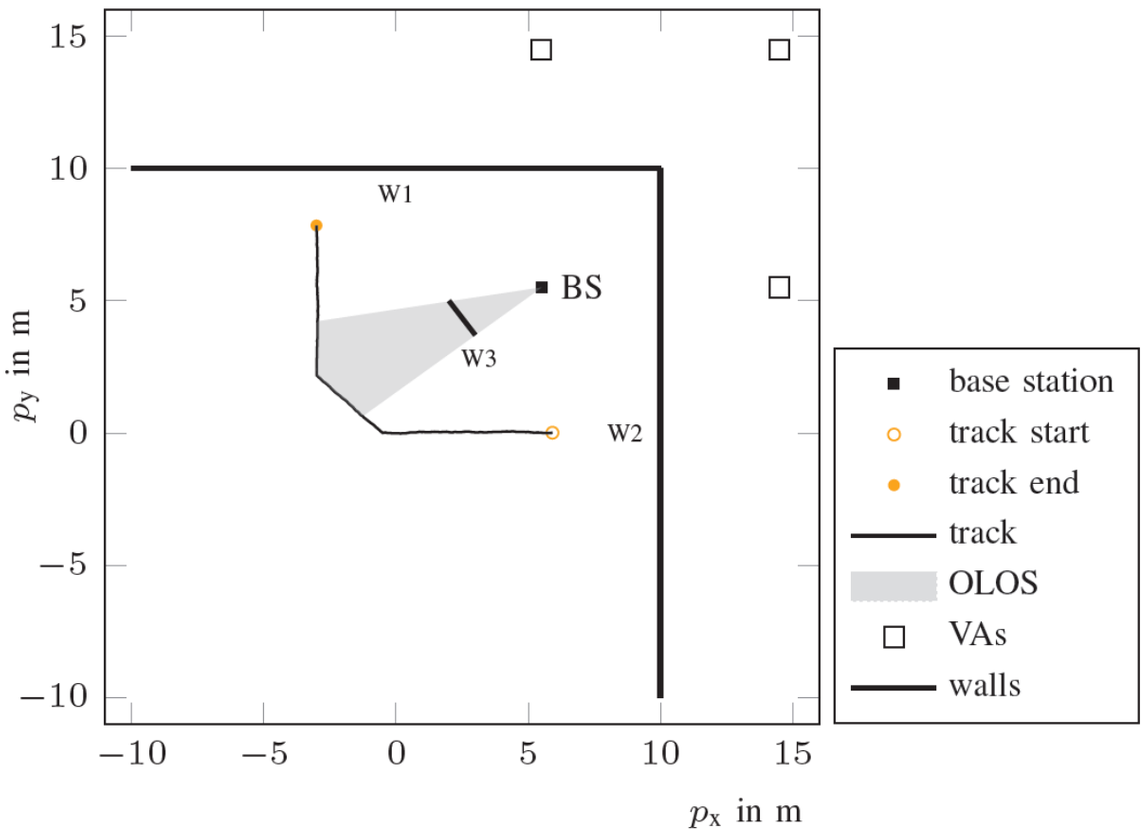

- Gray area: full obstruction to PA
- Agent RMSE along track
- Comparison:
  - Algorithm that uses only LOS
  - Benchmark: Algorithm that perfectly knows map